CHAPTER (8)

CONCLUSIONS

&

SUGGESTIONS FOR FUTURE WORK

8.1 Conclusions

Testing woven-roving GFRE specimens, with $[0,90°]_{3s}$ and $[\pm45°]_{3s}$ fiber orientations with two method of manufacturing M_1 and M_2 for each orientation, under pure bending, pure torsion, hydrostatic internal pressure and combined completely reversed bending moment and internal pressure, with different pressure ratios resulted in the following conclusions:

1. Specimens under static bending and completely reversed pure bending moment with fiber orientation $[0,90°]_{3s}$ and method of manufacturing M_2 have higher bending strength than the other specimens with $[\pm45°]_{3s}$ fiber orientation and method of manufacturing M_1, while specimens under static torsional and completely reversed torsional moment, the fiber orientation $[\pm45°]_{3s}$ and method of manufacturing M_1 have higher torsional strengths than other specimens with $[0,90°]_{3s}$ fiber orientation and M_2 method of manufacturing, However, under static pressure tests, the $[\pm45°]_{3s}$ fiber orientation and M_2 method of manufacturing specimens have the higher burst pressure than the other specimens.

2. Using the power formula:$\sigma_{max} = aN^b$ has proved its suitability for present study, and it is found that, the deviation of the constant (b) for different pressure ratios (Pr) and fiber orientations is negligible and it may be considered to be constant.

3. The value of the constant (a) was found to be depend on the fiber orientation angle (θ) and the pressure ratio (P_r) with high correlation factors, as the pressure ratio (P_r) or the fiber orientation increases the value of (a) will decreases, i.e. the pressure ratio (P_r) and the fiber orientation had a detrimental effect on the fatigue strength.

4. For the method of manufacturing M_2, the values of constant (a) are higher than that for the method of manufacturing M_1.

5. The new form of Goodman's equation for the case of combined completely reversed bending moment and hydrostatic internal pressure $\left\{\frac{\sigma_H}{S_H}+\frac{\sigma_{max}}{S_f}=1.0\right\}_{\theta,P_r,M}$ was found to be suitable for representing the effect of mean stress for present work.

6. The new form of SWT* parameter ($\sqrt{(\sigma_{max}+\sigma_m)(\sigma_a+K\sigma_h)}$), is valid for GFRE for all fiber orientation under completely reversed pure bending and hydrostatic pressure. Using power formula $\boldsymbol{SWT^*=a_1N^{b_1}}$ has resulted in having a nearly constant ratio between (a_1) and the corresponding static strength for both fiber orientations and both method of manufacturing M_1 and M_2. Performing only the completely reversed (R=-1) fatigue test and using SWT* parameter will be sufficient to find out the strength of the material.

7. The modified SWT parameter ($K_{Wafa}\sqrt{(\sigma_{max}+\sigma_m)(\sigma_a+K\sigma_h)}$) is equal to 0.25489 and valid for Woven-roving GFRE for both fiber orientations and both method of manufacturing under combined completely reversed bending moment and hydrostatic internal pressure..

8. The modified fatigue strength ratio (Ψ) has become a useful measure for establishing the master S-N relationship for Woven-roving GFRE for both fiber orientations and both method of manufacturing M_1 and M_2 under combined completely reversed bending moment and hydrostatic internal pressure over a range of pressure ratios.

9. A new form of failure criteria was introduced to govern the fatigue behavior of present study.

8.2 Suggestions for Future Work

Some points are still required to be examined, in future, to complete the related topics to this work. These points may be summarized as follows:

1. Study the fatigue behavior for woven-roving GFRE under combined completely reversed torsion and hydrostatic internal pressure with different pressure ratios.
2. Study the fatigue behavior for woven-roving GFRE under combined completely reversed bending moment and fluctuating internal pressure with different pressure ratios.

3. Study the fatigue behavior for woven-roving GFRE under combined bending and /or torsion (in-phase and out-phase) and hydrostatic internal pressure with different stresses and pressure ratios.
4. The effect of unsymmetrical fiber layers under combined bending and /or torsion and internal pressure should also be examined.
5. Study the fatigue behavior for woven-roving GFRE under combined completely reversed bending and hydrostatic internal pressure with different types of materials and specimens stacking.

REFERENCES

[1] Kaw A. K., Mechanics of Composite Materials, Second Edition, Taylor and Francis Group, Boca Raton, 2005.

[2] Broutman L. J. and Krock R. H., Modern Composite materials, Volume 2, Edited by Sendeckyj G. P., Academic Press, New York, 1974, www.books.google.com

[3] Pandey P. C., Introduction to Composite Materials, Syllabus Version 2.0, Department of Civil Engineering, IISc Bangalore, 17 August 2004.

[4] Reddy J. N., Mechanics of Laminated Composite Plates and Shells: Theory and Analysis 2nd Ed, CRC Press, 2004.

[5] Knops M. and Bogle C. Gradual failure in fiber/polymer laminates. Composites Science and Technology, 2005.

[6] Jang B. Z. Advanced Polymer Composites: Principal and Applications. ASM International, Materials Park, OH, 1994, www.books.google.com

[7] Daniel I. M. and Ishai O., Engineering Mechanics of Composite Materials, 2Ed. Oxford University Press., Inc. 2006.

[8] Onder A., First Failure Pressure of Composite Pressure Vessels. Graduate School of Natural & Applied Sciences of Dokuz Eylul University, 2007.

[9] Gay D., Hoa S. V. and Tsai S. W., Composite Materials Design and Applications, CRC Press LLC, New York, 2003.

[10] Fahrer A., A Study of the Manufacturing and Characterisation of Filament Wound Reinforced Thermoplastic Pipework, PhD Thesis, University of Newcastle, 1997.

[11] Gibson A. G., Composite materials in the offshore industry, Metals and materials, 1989, Vol.5, No.10, pp. 590-594.

[12] Gibson A. G. and Spagni D. A., Recent developments in the use of composite materials offshore, in the proceeding of a conference on polymers in Marine Environment, The Institute of Marine Engineers (UK), 1991, pp.3-9.

[13] Salama M. M., Advanced composites for the offshore industry: applications and challenges, Revue de Institute Francis du Petrole, 1995, 50 (1), pp.19-26, www.books.google.com

[14] Frost S. R., Applications of polymer composites within the oil industry, Composites for the Offshore Oil and Gas Industry - Design and Application, 1999, pp.45-54.

[15] Lye S. W. and Boey F. Y. C., Development of a low-cost prototype filament-winding system for composite components. Journal of Materials Processing Technology, 1995, 52(2-4), pp. 570-584.

[16] Rreifsnider K. L., Henneke E. G., Stinchcomb W. W. and Duke J. C., Damage Mechanics and NDE of composite Laminates. In: Hashin Z, Herakovich CT, editors. Mechanics of Composite Materials. Recent advances. New York: Pergamon Press, 1983. pp. 399-420.

[17] Hull D., Legg M. J., and Spencer B., Failure of glass/polyester filament wound pipe. Composites, 1978, 9(1), pp.17-24.

[18] Soden P. D., Kitching R., and Tse P. C., Experimental failure stresses for ±55° filament wound glass fibre reinforced plastic tubes under biaxial loads. J. of Composites, 1989, 20(2), pp.125-135.

[19] Broutman L. J. and Sahu S., Progressive Damage of a Glass Reinforced Plastic during Fatigue, SPI, 24th Annual Technical Conference, Washington D.C., 1969, Section 11-D.

[20] Garrett K. W. and Bailey J. E., Multiple transverse fracture in 90° cross-ply laminates of a glass fibre-reinforced polyester, Journal of Materials Science, 1977, 12(1), pp. 157-168.

[21] Highsmith A. L. and Reifsnider K. L., Stiffness reduction mechanisms in composite laminates, Damage in composite materials, 1982, ASTM STP 775, pp. 103-117.

[22] Harrison R. P. and Barder M. G., Damage development in CFRP laminates under monotonic and cyclic stressing. Journal of Fibre Science and Technology, 1983, 18(3), pp.163-180.

[23] Nairn J. A. and Hu S., The initiation and growth of delaminations induced by matrix microcracks in laminated composites, International Journal of Fracture, 1992, 57(1), pp. 1-24.

[24] Nairn J. A., Hu S., and Bark J. S., A critical evaluation of theories for predicting microcracking in composite laminates, Journal of Materials Science, 1993, 28(18), pp. 5099-5111.

[25] Katerelos D. G., McCartney L. N., and Galiotis C., Effect of off - Axis matrix cracking on stiffness of symmetric angle-ply composite laminates, International Journal of Fracture, 2006, 139(3-4), pp. 529-536.

[26] Katerelos D. G., Lundmark P., Varna J., Galiotis C., Analysis of matrix cracking in GFRP laminates using Raman spectroscopy, Journal of Composites Science and Technology, 2007, 67(9), pp. 1946-1954.

[27] Tao J. X. and Sun C. T., Effect of matrix cracking on stiffness of composite laminates, Journal of Mechanics of Composite Materials and Structures, 1996, 3(3), pp. 225-239.

[28] Sun C. T. and Tao J. X., Prediction of failure envelopes and stress/strain behaviour of composite laminates, Journal of Composites Science and Technology, 1998, 58(7), pp. 1125-1136.

[29] Jones R. M., Mechanics of Composite Materials, McGraw-Hill Inc. 1975.

[30] Bailey J. E., Parvisi A., On fibre debonding effects and the mechanism of transverse-ply failure in cross-ply laminates of glass fibre/thermoset composites, Journal of Materials Science, 1981, b16 (3), pp. 649-659.

[31] Gemi L., Tarakcioglu N., Akdemir A.,Sahin O. S., Progressive fatigue failure behavior of glass/epoxy $(\pm 75)_2$ filament-wound pipes under pure internal pressure, Journal of Materials and Design, 2009, 30(10), pp. 4293-4298.

[32] Frost S.R., Predicting the long term fatigue behaviour of filament wound glass/epoxy matrix pipes, Proceeding of the 10th international Conference of Composite Materials (ICCM 10), 1995, (1), pp. 649-656.

[33] Frost S. R., Design, Failure and Life Predictions of Composite Pipelines and Piping Systems. SIEP B. V., 1997.

[34] Jones M. L. C. and Hull D., Microscopy of failure mechanisms in filament-wound pipe, Journal of Materials Science, 1979, 14(1), pp. 165-174.

[35] Meijer G. and Ellyin F., A failure envelope for ±60° filament wound glass fibre reinforced epoxy tubular, Journal of Composites Part A: Applied Science and Manufacturing, 2008. 39(3), pp. 555-564.

[36] Ellyin F., Carroll M., Kujawski D. and Chiu A. S., The behavior of multidirectional filament wound fibre glass/epoxy tubulars under biaxial loading, Journal of Composites Part A: Applied Science and Manufacturing, 1997. 28(9-10), pp. 781-790.

[37] O'Brien T. K. Analysis of local delaminations and their influence on composite laminate behavior in ASTM Special Technical Publication. 1985, http://www.google.com.eg/books

[38] Wang A. S. D., Kishore N. N., and Li C. A., Crack development in graphite-epoxy cross-ply laminates under uniaxial tension, Journal of Composites Science and Technology, 1985, 24(1), pp. 1-31.

[39] Hashin Z., Fatigue Failure Criteria for Unidirectional Fibre Composites, Journal of Applied Mechanics, 1981, 48, pp. 846-852.

[40] Nagendra V. A. and Talreja R., A mechanistic model for fatigue damage evolution in composite laminates, Journal of Mechanics of Materials, 1998, 29, pp. 123-140.

[41] Takeda N. and Ogihara S., Initiation and growth of delamination from the tips of transverse cracks in CFRP cross-ply laminates, Journal of Composites Science and Technology, 1994, 52(3), pp. 309-318.

[42] Kashtalyan M. and Soutis C., Effect of delaminations induced by transverse cracks and splits on stiffness properties of composite laminates, Journal of Composites Part A: Applied Science and Manufacturing, 2000, 31(2), pp. 107-119.

[43] Noh J. and Whitcom J., Effect of delaminations on opening of transverse matrix cracks, Journal of Composite Materials, 2005, 39(15), pp. 1353-1370.

[44] Majid M. S. A. , Assaleh T. A., Gibson A. G., Hale J. M., Fahrer A., Rookus C. A. P. and Hekman M., Ultimate elastic wall stress (UEWS) test of glass fibre reinforced epoxy (GRE) pipe, Journal of Composites: Part A, 2011, 42, pp. 1500–1508.

[45] Pabiot J., Krawczak P., and Monnier C., Behaviour of Glass-Fibre Composite Pipes under Internal Pressure as a Function of Composite Cohesion Parameters, 49th Annual Conference. Composite Institute, The Society of the Plastic Industry, Inc., 1994, pp. 7-9.

[46] Mieras H. J. M. A., Irreversible Creep of Filament-Wound Glass-Reinforced Resin Pipes. Journal of Plastics & Polymers, 1973, 41, pp. 84-88.

[47] Legg M. J. and Hull D., Effect of resin flexibility on the properties of filament wound tubes, Journal of Composites, 1982, 13(4), pp. 369-376.

[48] Tanigushi K., Ohira M., and Ishii M., The Effect of Matrix Resins on the Mechanical Properties of Fibre glass Reinforced Pipes for Oil and Gas Production,

46th Annual Conference. Composite Institute, The Society of the Plastics Industry, Inc., 1991, pp. 18-21.

[49] Orifici A. C., Herszberg I., and Thomson R.S., Review of methodologies for composite material modelling incorporating failure, Journal of Composite Structures, 2008, 86(1-3), pp. 194-210.

[50] Spencer B. and Hull D., Effect of winding angle on the failure of filament wound pipe, Journal of Composites, 1978, 9(4), pp. 263-271.

[51] Parnas L. and Katırc N., Design of fiber-reinforced composite pressure vessels under various loading conditions, Journal of Composite Structures, 2002, 58, pp.83‑95.

[52] Dogan T., Prediction of Composite Vessels Under Various Loadings, Master Thesis, 2006, Dokuz Eylul University, Department of Mechanical Engineering, Izmir, Turkey.

[53] Sinha M. and Pandit S. N., Design and Burst Pressures Analysis of CFRP Composite Pressure Vessel for Various Fiber Orientations Angles, International Journal of Advances in Engineering Science and Technology, 2012, 1 (1), PP.35-40, ISSN /IJAEST/V1N1.

[54] Martins L. A., Bastian F. L. and Netto T. A., Structural and functional failure pressure of filament wound composite tubes, Journal of Materials and Design, 2012, 36, pp.779–787.

[55] Hale J.M., Gibson A.G., and Speake S.D., Biaxial failure envelope and creep testing of fibre reinforced plastic pipes in high temperature aqueous environments, Journal of Composite Materials, 2002, 36(3), pp. 257-270.

[56] Carroll M., Ellyin F., Kujawski D. and Chiu A. S., Rate-dependent behaviour of ±55° filament-wound glass-fibre/epoxy tubes under biaxial loading, Journal of Composites Science and Technology, 1995. 55(4), pp. 391-403.

[57] Roberts S. J., Evans J. T. and Gibson A. G., The effect of matrix microcracks on the stress-strain relationship in fiber composite tubes, Journal of Composite Materials, 2003. 37(17), pp. 1509-1523.

[58] Soden P. D., Kitching R., Tse P. C., Tsavalas Y. and Hinton M. J., Influence of winding angle on the strength and deformation of filament-wound composite tubes

subjected to uniaxial and biaxial loads, Journal of Composites Science and Technology, 1993, 46(4), pp. 363-378.

[59] Soden P. D., Leadbetter D., Griggs, P. R. and Eckold, G. C., The strength of a filament wound composite under biaxial loading. Journal of Composites, 1978. 9(4), pp. 247-250.

[60] Dharan, C. K. H., The Fatigue Behavior of Fiber-Reinforced Polymers and Advanced Composites", ASME Design Engineering Conference, ASME Paper No. 77-DE-41, American Society of Mechanical Engineers (Paper), New York, 1977.

[61] Owen M. J. and Griffiths J. R., Evaluation of biaxial stress failure surfaces for a glass reinforced polyester resin under static and fatigue loading, Journal of Materials Science, 1978. 13, pp. 1521-1537.

[62] Bredemo R., Damage development during uniaxial fatigue of filament wound tubes, SICOM report 92-001. Pitea (Sweden): Swedish Institute of composites, 1992.

[63] Perreux D. and Joseph E., The effect of frequency on the fatigue performance of filament-wound pipes under biaxial loading: Experimental results and damage model, Journal of Composites Science and Technology, 1997, 57(3), pp. 353-364.

[64] Rousseau J., Perreux D., and Verdiere N., The influence of winding patterns on the damage behaviour of filament-wound pipes, Journal of Composites Science and Technology, 1999. 59(9), pp. 1439-1449.

[65] Kaynak C. and Mat O., Uniaxial fatigue behavior of filament-wound glass-fiber/epoxy composite tubes, Journal of Composites Science and Technology, 2001, 61(13), pp. 1833-1840.

[66] Tarakcioglu N., Gemi L., and Yapici A., Fatigue failure behavior of glass/epoxy ±55 filament wound pipes under internal pressure, Journal of Composites Science and Technology, 2005, 65(3-4), pp. 703-708.

[67] Duggan T. V. and Byrne J., Fatigue as a Design Criterion, McMillan Press Ltd., 1977 (ISBN: 0-333-21488-9).

[68] Kim H. C. and Ebert L. J., Axial Fatigue Failure Sequence and Mechanisms in Unidirectional Fiber glass Composite, , Journal of Composite Material, 1978, 12, pp.139-152.

[69] Wang S. S., Chim E. S. M., Socie D. F., Gauchel J. V., and Olinger J. L., Tensile and Torsional Fatigue of Fibre-reinforced Composites at Cryogenic Temperatures, , Journal of Engineering Materials and Technology, 1982, 104, pp. 121-127.

[70] Yang B., Kozey V., Adanur S. and Kumar S., Bending, Compression, and Shear Behavior of Woven Glass Fiber-Epoxy Composite, , Journal of Composites: part B, 2000, 31, pp.715-721.

[71] Mahfouz H., Response of Resin Transfer Moulded (RTM) Composites Under Reversed Cyclic Loading, , Journal of Engineering Materials & Technology, 1996, 118, pp. 49-57.

[72] Amijima S., Fujii T. and Sagami T., Non-Linear Behavior of Plain Woven G.F.R.P Under Repeated Biaxial Tension/Torsion Loading, In Proceeding of the thirteenth annual energy-sources technology conference and exhibition, New Orleans, LA, January 14-18, 1990, pp.261-266.

[73] Krempl E., Elzey D. M., Hong B. Z., Ayar T., and Loewy R. G., Uniaxial and Biaxial fatigue Properties of Thin-Walled Composite Tubes, Journal of the American Helicopter Society, 1988 August,33(3), pp. 3-10.

[74] Abouelwafa M. N., Hamdy A. H. and El-Midany A. A., Combined Bending and Torsion of Woven Roving GRP, Alexandria Engineering Journal, Trans ASME, 1997, 119, pp.180-185.

[75] Ahmed M. E. and Khashaba U. A., Fatigue analysis of Unidirectional GFRP Composite Under Combined Bending and Torsional Loads, Journal of Composite Structure, 2006, 79, pp.599-605.

[76] Hashin Z., Fatigue Failure Criteria for Unidirectional Fibre Composites, Journal of Applied Mechanics, 1981, 48, pp. 846-852.

[77] Francis P. H., Biaxial Fatigue Loading of Notched Composites, Journal of Composite Materials, 1977, 11, pp.488-499.

[78] Ellyin F. and Kujawski D., Fatigue testing and life prediction of fiber glass-reinforced composites. In: Neale K.W. and Labossière P. (eds.), First International Conference on Advanced Composite Materials in Bridges and Structures (ACMBS-I), 1992, Sherbrooke, Québec, Canada, Canadian Society for Civil Engineering, pp. 111-118.

[79] Kujawski D. and Ellyin F., Rate/Frequency-Dependent behaviour of fiberglass/epoxy laminates in Tensile and cyclic Loading, Journal of Composites, 1995, 26(10), pp.719-723.

[80] Lee B. L. and Liu D. S., Cumulative Damage of Fiber-Reinforced Elastomer Composites Under Fatigue Loading, Journal of Composite Materials, 1994, 28(13), pp.1261-1286.

[81] Farrow I. R., Damage accumulation and degradation of composite laminates under aircraft service loading: assessment and prediction, Volumes I and II, Cranfield Institute of Technology, PhD Thesis, 1989.

[82] Chamis C. C., Mechanics of Load Transfer at the Fiber/Matrix Interface, NASA TN D-6588, February 1972.

[83] El-Midany A. A., Fatigue of Woven-Roving Glass Fiber Reinforced Polyester Under Combined Bending and Torsion, PhD. Thesis, Alexandria University, Egypt, 1995.

[84] Nasr M. A., The Effect of Mean Stress on the Fatigue Behaviour of Woven-Roving GFRP Subjected to Torsional Moments, MSc. Thesis, Alexandria University, Egypt, 2002.

[85] Sharara A. I., Effect of Stress Ratio on Fatigue Characteristics of Woven-Roving Glass Reinforced Polyester, MSc. Thesis, Alexandria University, Egypt, 1997.

[86] El-hadary M. M., Fatigue Behaviour of Woven-Roving GFRP Under Combined Bending and Torsion Moments with Different Fluctuating Stresses, MSc. Thesis, Alexandria University, Egypt, 2006.

[87] El-hadary M. M., Fatigue Behaviour of Woven-Roving Glass Reinforced Polyester Under Combined Out-of-Phase Bending and Torsion Moments with Different Fluctuating Stresses, PhD. Thesis, Alexandria University, Egypt, 2011.

[88] Mohamed Y. S., A Study the Effect of Fiber Orientation and Negative or Positive Stress Ratios on Fatigue Characteristics of Woven-Roving Glass Reinforced Polyester Under Combined Bending and Torsional Moments, PhD. Thesis, Alexandria University, Egypt, 2011.

[89] Soden P.D., Kitching R., Tse P. C., Tsavalas Y. and Hinton M. J., Influence of winding angle on the strength and deformation of filament-wound composite tubes

subjected to uniaxial and biaxial loads, Journal of Composites Science and Technology, 1993, 46(4), pp. 363-378.

[90] Rosenow M. W. K., Wind angle effects in glass fibre-reinforced polyester filament wound pipes, Journal of Composites, 1984, 15(2), pp. 144-152.

[91] Mistry J., Theoretical investigation into the effect of the winding angle of the fibres on the strength of filament wound GRP pipes subjected to combined external pressure and axial compression, Journal of Composite Structures, 1992, 20(2), pp. 83-90.

[92] Moreno H., Douchin B., Collombet F., Choqueuse D. and Davies P., Influence of winding pattern on the mechanical behavior of filament wound composite cylinders under external pressure, Journal of Composites Science and Technology, 2008, 68(3-4), pp. 1015-1024.

[93] Mertiny P., Ellyin F. and Hothan A., An experimental investigation on the effect of multi-angle filament winding on the strength of tubular composite structures, Journal of Composites Science and Technology, 2004, 64(1), pp. 1-9.

[94] Lea R. H. and Yang C., Improving the mechanical properties of composite pipe using multi-axial filament winding, Proc. of NACE Annual Conference Corrosion, 1998, pp. 458/1-458/6.

[95] Gerber H. Bestimmung der zulassigen Spannungen in Eisen-konstruction. Zeitschrift des Bayerischen Architeckten und Ingenieur-Veriens 1984, 6, pp.101-110.

[96] Abouelwafa M. N., Gomaa A., Hamdy A., Morsi E. and Nasr M. A., The effect of mean stress on the fatigue behaviour of woven-roving GFRP subjected to torsional moments, Alexandria Engineering Journal, 2005, 44 (1), pp.9-18.

[97] El Kadi H., and Ellyin F., Effect of Stress Ratio on the Fatigue of Unidirectional Fibre glass-Epoxy Composite Laminae, Journal of Composite Material, 1994, 25(10), pp. 917-924.

[98] Fujii T., Shiina T. and Okubo K., Fatigue Notched Sensitivity of Glass Woven Fibric Composites Having A Circular Hole Under Tension/Torsion Biaxial Loading, Journal of composite Materials, 1994, 28, pp.234-251.

[99] Bradely L., Model Determined for Predicting Fatigue Lives of Metal Matrix Composites under Mean Stresses, www.grc.nasa.gov.

[100] Dalmeida J. R. M., de Almeida R. C. and de Lima W. R., Effect of water absorption of the mechanical behavior of fiberglass pipes used for offshore service waters, Journal of Composite Structures, 2008, 83, pp. 221–225.

[101] Zamri M. H., Akil H. M., Abu Bakar A., Ishak Z. A. M. and Wei Cheng L., Effect of water absorption on pultruded jute/glass fiber-reinforced unsaturated polyester hybrid composites, Journal of Composite Materials, 2011, 46(1), pp.51–61.

[102] Athijayamani A., Thiruchitrambalam M., Natarajan U. and Pazhanivel B., Effect of moisture absorption on the mechanical properties of randomly oriented natural fibers/polyester hybrid composite, Journal of Materials Science and Engineering A, 2009, 517, pp.344–353.

[103] Merah N., Nizamuddin S., Khan Z. and Al-Sulaiman F, Effects of harsh weather and seawater on glass fiber reinforced epoxy composite, Journal of Reinforced Plastics and Composites, 2010, 29(20), pp.3104–3110.

[104] Schutte C. L., Environmental durability of glass-fiber composites, Journal of Materials Science and Engineering R: Reports, 1994, 13(7), pp. 265-324.

[105] Lundgren J. E. and Gudmundson P., Moisture absorption in glass-fibre/epoxy laminates with transverse matrix cracks, Journal of Composite Science Technology, 1994, 59, pp. 1983-1991.

[106] Kotsikos G., Evans J. and Hale J., Evaluation of effects of pre-exposure in marine environments of structural glass reinforced composites by acoustic emission testing. Journal of Material Evaluation, 2000, 58, pp. 1320-1325.

[107] Komai K., Minoshima K., Shibutai T. and Nomura T., The Influence of Water on the Mechanical Properties and Fatigue Strength of Angle-Ply Carbon/Epoxy Composites, JSME Int, J. series 1, 1989, 32, pp. 588-595.

[108] Perreux D. and Suri C., A study of a coupling between the phenomena of water absorption and damage in glass/epoxy composite pipe, Journal of Composite Science Technology, 1997, 57, pp. 1403-1413.

[109] Vauthier E., Abry J. C., Bailliez T. and Chateauminois A., Interaction between hygrothermal ageing and fatigue damage in unidirectional glass/epoxy composites, Journal of Composites Science and Technology, 1998, 58, pp. 687-692.

[110] Ellyin F. and Rohrbacher C., Effect of aqueous environment and temperature on glass-fibre epoxy resin composites, Journal of Reinforced Plastics and Composites, 2000, 19(17), pp. 1405-1427.

[111] Ellyin F., Durability of glass-fibre reinforced polymer composites in aqueous and high temperature environments, Journal of Polymers and Polymer Composites, 2004, 12(4), pp. 277-288.

[112] Ellyin F. and Maser R., Environmental effects on the mechanical properties of glass-fiber epoxy composite tubular specimens, Journal of Composites Science and Technology, 2004, 64(12), pp. 1863-1874.

[113] Chiou P. L. and Bradley W. L., Moisture-induced degradation of glass/epoxy filament wound composite tubes, Journal of Thermoplastic Composite Materials 1996, 9(2), pp. 118-128.

[114] Hale J. M., Gibson A. G., and Speake S. D., Tensile strength testing of GRP pipes at elevated temperatures in aggressive offshore environments, Journal of Composite Materials, 1998, 32(10), pp. 969-986.

[115] Subramanian S., Elmore I. S., Stinchcomb W. W. and Reifsnider K. L., Influence of Fiber–Matrix Interphase on the long-Term Behavior of graphite/Epoxy Composite, In: Deo R. B., Saff C. R., editors, Composite material: Testing and Designe. ASTM STP 1274, American Society for Testing and Materials, 1996, 12, pp.69-87, www.books.google.com

[116] Azzi V. D. and Tsai S. W., Anisotropic strength of composites - Investigation aimed at developing a theory applicable to laminated as well as unidirectional composites, employing simple material properties derived from unidirectional specimens alone, Journal of Experimental Mechanics, 1965, 5(9), pp. 283-288.

[117] Tsai S. W. and Wu E. M., A General Theory of Strength for Anisotropic Materials, Journal of Composite Materials, 1971, 5, pp. 58-80.

[118] Hanh H. T. and Tsai S. W., On the behaviour of composite laminates after initial failures, Journal of Composite Materials, 1974, 8, pp. 280-305.

[119] Hinton M. J. and Soden P. D., Predicting failure in composite laminates: the background to the exercise, Journal of Composites Science and Technology, 1998, 58(7), pp. 1001-1010.

[120] Puck A. and Schneider W., On Failure Mechanisms and Failure Criteria of Filament Wound Glass Fibre/Resin Composites, Journal of Plastics & Polymers, 1969, 37, pp. 270-273.

[121] Sim D. F. and Brogdon V. H., Fatigue behaviour of composites under different loading modes. Fatigue of Filamentary materials, ASTM STP 636, 1977, pp. 185-205, www.books.google.com

[122] Philippidis T. P. and Vassilopoudos A. P., Fatigue strength prediction under multiaxial stress, Journal of Composite Materials, 1999, 33(17), pp. 1578-1599.

[123] Hashin Z., Failure Criteria for Unidirectional Fibre Composites, Journal of Applied Mechanics, 1980, 47, pp. 329-334.

[124] Rotem A., Prediction of laminate failure with the Rotem failure criterion, Journal of Composites Science and Technology, 1998, 58(7), pp. 1083-1094.

[125] Smith K.N, Watson P. and Topper T.H, A Stress-Strain Function for the Fatigue of Metals, Journal of Materials, 1970, 5, pp.767-778.

[126] Conle A. and Ingall J.P., Effects of Mean Stress on the Fatigue of Composite Materials, Journal of Composites Technology & Research, 1985, 7, Spring, pp. 3-11.

[127] Sauer J.A., McMaster A.D., and Morrow D.R., Fatigue Behaviour of Polystyrene and Effects of Mean Stress, Journal of Macro-Molecular Science-Physics, 1976, 812 (4), pp. 535-562.

[128] Ryder J.T. and Walker E.K., Effects of Compression on Fatigue Properties of Quasi - Isotropic Graphite / Epoxy Composite, Fatigue of Filamentary Composite, ASTM STP 638, Materials American Society for Testing and Materials, Philadelphia, 1977, pp. 3- 26.

[129] Smith T.R. and Owen M.J., Fatigue Properties of RP, Journal of Plastics, 1969 April, 46, pp. 121-129.

[130] Schuetz D. and Gerharz E.J., Fatigue Strength of a Fibre-Reinforced Material, Journal of Composites, 1977, 8 (4), pp. 245-254.

[131] Ramani S.V. and Williams D.P., Axial Fatigue [0,30°] Graphite / Epoxy, In: Failure Modes in Composites III, The Metallurgical Society of the ASME, New York,1976, pp. 115-140.

[132] Sturgeon J.B. and Rhodes F.S, The fatigue of ±45° Carbon Fibre Reinforced Plastics, Royal Aeronautical Establishment Technical Report, September, 1980.

[133] Gravett P.W., A Life Prediction Method for Matrix Dominated Fatigue Failures of SCS-6/Ti-15-3 MMC", Reliability, Stress Analysis, and Failure Prevention, DE-American Society of Mechanical Engineers, New York, 1993, 55, pp. 223-230.

[134] Basquin OH., The exponential law of endurance test, ASTM, 1980, 10, pp. 625-630.

[135] Awerbuch J. and Hahn HT., off-axis fatigue of graphite/epoxy composite, ASTM STP 723, 1981, pp.243-273.

[136] Kawai M., A phenomenological model for off-axis fatigue behavior unidirectional polymer matrix composites under different tress ratios, Journal of Composite Materials Part A, 2004, 35, pp. 955-963.

[137] Landgraf RW., The resistance of metals to cyclic deformation, ASTM; STP 467, 1970, pp. 3-36.

[138] Mohamed M. Y., The Inclusion Effect on the Fatigue Behaviour of Woven-Roving GRP Composite Materials, MSc. Thesis, Alexandria University, Egypt, 2001.

[139] Highton J., Adeoye A. B., and Soden P. D., Fracture Stresses for ± 75 Degree Filament Wound GRP Tubes under Biaxial Loads, Journal of Strain Analysis for Engineering Design, 1985, 20(3), pp. 139-150.

[140] Tarakcioglu N., Gemi L. and Yapici A., Fatigue failure behavior of glass epoxy± 55 filament wound pipes under internal pressure, Journal of Composites Science and Technology, 2005, 65, pp. 703–708.

[141] Lees J. M., Behaviour of GFRP adhesive pipe joints subjected to pressure and axial loadings, Journal of Composites: Part A, 2006, 37, pp. 1171–1179.

[142] Tarakcioglu N., Samanci A., Arikan H. and Akdemir A., The fatigue behavior of $(\pm 55°)_3$ filament wound GRP pipes with a surface crack under internal pressure, Journal of Composite Structures, 2007, 80, pp. 207-211.

[143] Mertiny P. and Gold A., Quantification of leakage damage in high-pressure fibre-reinforced polymer composite tubular vessels, Journal of Polymer Testing, 2007, 26, pp. 172-179.

[144] Gemi L., Tarakcioglu N., Akdemir A. and Sahin O. S., Progressive fatigue failure behavior of glassepoxy (±75º)2 filament-wound pipes under pure internal pressure, Journal of Materials and Design, 2009, 30, pp. 4293–4298.

[145] Arikan H., Failure analysis of $(\pm 55^{o})_3$ filament wound composite pipes with an inclined surface crack under static internal pressure, Journal of Composite Structures, 2010, 92, pp. 182–187.

[146] Abouelwafa M. N., Hamdy A. H. and Showaib E. A., A New Testing Machine for Fatigue Under Combined Bending and Torsion Acting Out-of-Phase, Alexandria Engineering Journal, 1996, 28(4), pp.113-95.

[147] Mohamed Y. S. and Graduation project groups, Composite Materials, Fatigue Testing and Molding Machines, Graduation Project, Mechanical Engineering Department, Alexandria University, Alexandria, Egypt, 2012.

[148] Erkal S., Fatigue Damage in Composite Cylinders, PhD Thesis, 2007, Dokuz eylul University, Graduate School of Natural and Applied Sciences, Izmir, Turkey.

[149] Shigley J.E., Mechanical Engineering Design, McGraw-Hill, (ISBN: 0-07-056898-7), 1986.

[150] Myeong M., Kim Y. and Budden J. P., Limit load interaction of cracked branch junctions under combined pressure and bending, Journal of Engineering Fracture Mechanics, 2012, 86, pp. 1–12.

[151] Atcholi K. E., Oytana C., Varchon D., and Perreux D., Superposed Torsion-Flexure of Composite Materials: Experimental Method & Examples of Applications, Journal of Composite Materials, September 1992, 23, pp. 327-333.

[152] Kawakami H, Fujii T. and Morita Y., Fatigue degradation and life prediction of glass fabric polymer composite under tension/torsion biaxial loadings, Journal of Reinf. Plast. Composites, 1996, 15, pp.183–95.

[153] Demuth H. and Beale M., Neural Network Toolbox User's Guide for use with MATLAB Version 4.0, The Math Works, Inc. 2000.

[154] Helmy A. A., An expert system for life prediction of woven roving glass fiber reinforced polyester under cyclic bending loading, Alexandria Engineering Journal, 2004, 43(5), pp.621-629.

[155] Artymiak P., Bukowski L., Feliks J., Narberhaus S. and Zenner H., Determination of S-N curves with the application of artificial neural networks, Journal of Fatigue Fracture Eng. Material Structure, 1999, 22, pp.8:22.

[156] Venkatesh V. and Rack H.J., A neural network approach to elevated temperature creep-fatigue life prediction. Int. International Journal of Fatigue, 1999, 23, pp. 21-34.

[157] Pleune T.T. and Chopra O.K., Using artificial neural networks to predict the fatigue life of carbon and low-alloy steels. Nucl. Eng. Des, 2000,197, pp.1-12.

[158] Lee J. A., Almond D. P. and Harris B., The Use of Neural Networks for the Predication of Fatigue Lives of Composite Materials, Journal of Composites Part A: Applied Science and Manufacturing, 1999, 30 (10), pp. 1159-1169.

[159] Aymerich F. and Serra M., Predication of Fatigue Strength of composite Laminates by Means of Neural Networks, Key Engineering Materials, 1998, 144, pp. 231- 240 .

[160] Al-Assaf Y. and El-Kadi H., Fatigue Life Predication of Unidirectional Glass fiber/ Epoxy Composite Laminate Using Neural Networks, Journal of Composite Structures, 2001, 53 (1), pp. 65-71.

[161] El-Kadi H. and Al-Assaf Y., Predication of the Fatigue Life of Unidirectional Glass fiber/ Epoxy Composite Laminate Using different Neural Networks Paradigms, Journal of Composite Structures, 2002, 55, pp. 239-246.

[162] Choi S. W., Song E. and Hahn H.T., Predication of Fatigue Damage Growth in Notched Composite Laminates Using an Artificial Neural Network, Journal of Composite Science and Technology, 2003, 63, (5), pp. 661-665.

[163] Chen, S., Cowan C. F. N., and Grant P. M., Orthogonal Least Squares Learning Algorithm for Radial Basis Function Networks, IEEE Transactions on Neural Networks, 1991, 2(2), pp. 302-309.

[164] http://www.mscdirect.com/industrialtools/mobil-hydraulic-oil.html, Date (11-10-2014)

APPENDIX (1)

SPECIMENS CODE

Specimens Nomenclature

Considering the manufacturing parameters, a designation system is developed for the tests. This system identifies the test specimens by the *Method of Manufacturing*, *Fiber orientation*, and *Test Plan*. The Method of Manufacturing is designated by the letter "M" followed by the numbers 1 or 2, which are assigned to the first method of specimen manufacturing *(one step molding*) and second method of specimen manufacturing *(Step by step molding)*, respectively. Fiber orientation is next, called by the letter "A" and followed by 1 or 2, which are the fiber angles of $[0,90°]_{3s}$ and $[\pm 45°]_{3s}$ respectively, remembering all the specimens of these fiber angles are reinforced with a three layers of hoop fiber orientation as the outermost layer. The last letter "T" specifies the test plan; it has three digits, the first one is followed by the numbers 0, 1 and 2, which are assigned to 1 stands for *Closed Cylinder condition* and 2 stands for *Open Cylinder condition* or 0 stands for *unpressurised Cylinder condition.* The next digit is followed by 1 or 2, which are the test type of *Static condition* and *Fatigue condition* test respectively. The latter is followed by the numbers 1, 2, 3 and 4, which are the load type of *bending load, torsion load, static internal pressure* and *combined load* respectively.

The three last numbers before the dash shows the *Serial Number* of the test specimen, they are depended on sections after the dash. For example, the specimen number 19 that is manufactured with *Step by step molding*, fiber reinforced at an angle configuration of $[\pm 45°]_{3s}$, and was tested at *Completely Reversed Bending plus Static Pressure Test (Closed Cylinder)*, is designated as ***WA019-M2A2T124***.

APPENDIX (2)

THE FAILURE MODES

A2.1 Completely Reversed Pure bending Test

Table A2.1: The failure modes of M_1, $[0,90°]_{3s}$ specimens under completely reversed pure bending

N	Failure modes
$10^3 \leq N \leq 10^4$	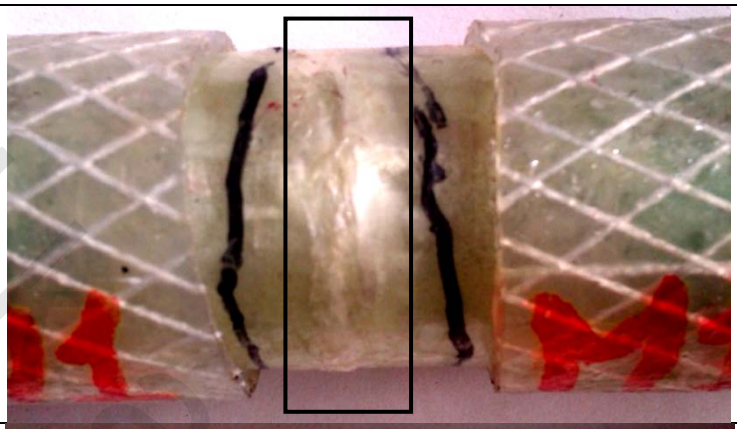
$10^4 \leq N \leq 10^5$	
$10^5 \leq N \leq 10^6$	

Table A2.2: The failure modes of M_2, $[0,90°]_{3s}$ specimens under completely reversed pure bending

N	Failure modes
$10^3 < N < 10^4$	
$10^4 < N < 10^5$	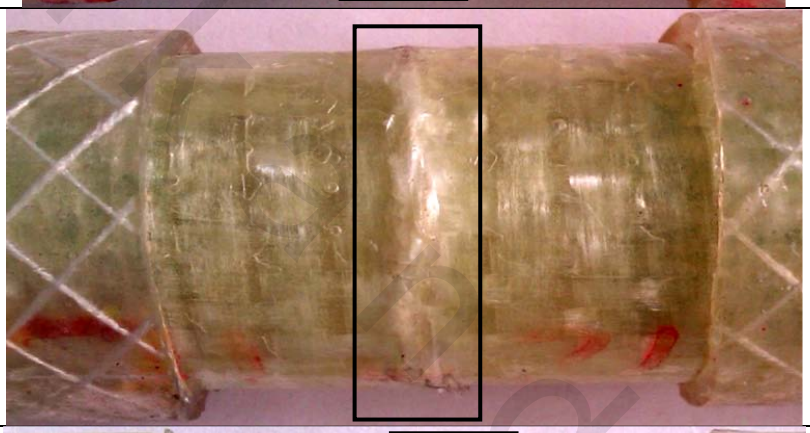
$10^5 < N < 10^6$	

Table A2.3: The failure modes of M_1, $[\pm 45°]_{3s}$ specimens under completely reversed pure bending

N	Failure modes
$10^3 < N < 10^4$	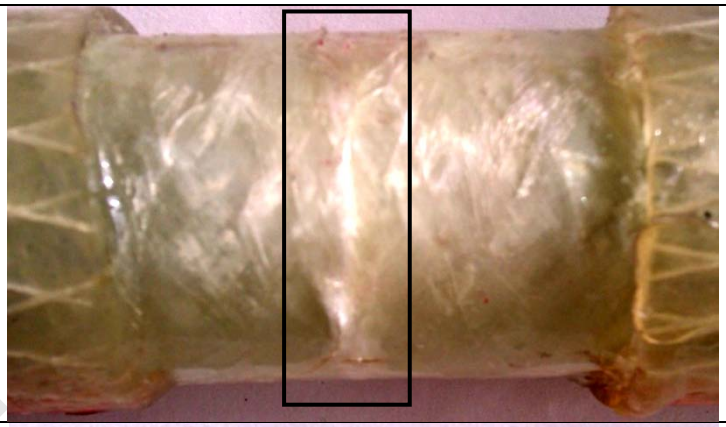
$10^4 < N < 10^5$	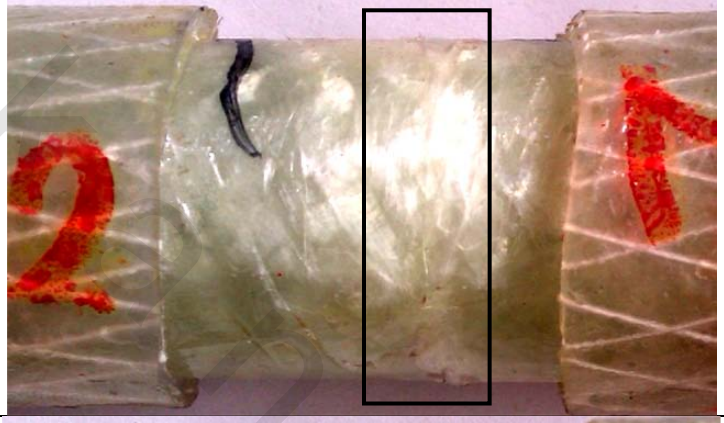
$10^5 < N < 10^6$	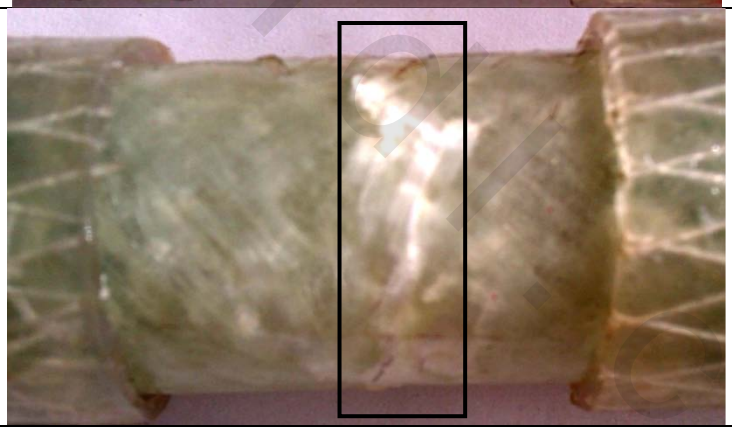

Table A2.4: The failure modes of M_2, $[\pm 45°]_{3s}$ specimens under completely reversed pure bending

N	Failure modes
$10^3 < N < 10^4$	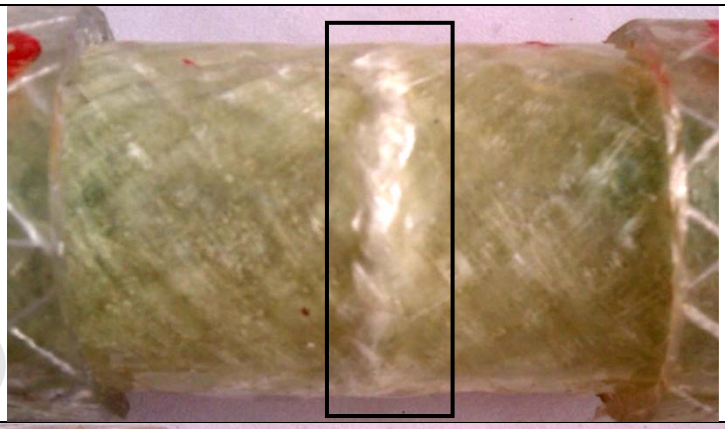
$10^4 < N < 10^5$	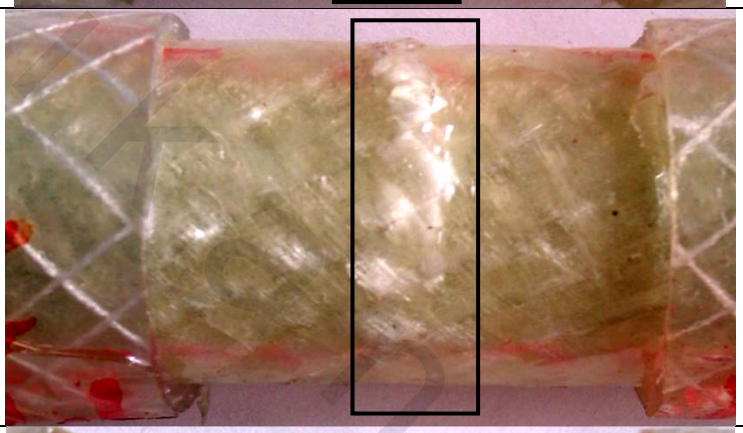
$10^5 < N < 10^6$	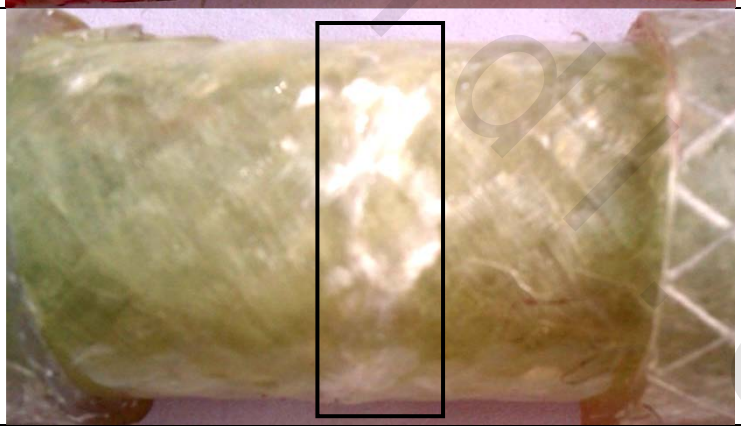

A2.2 Completely Reversed Pure Torsion Test

Table A2.5: The failure modes of M_1, $[0,90°]_{3s}$ specimens under completely reversed pure torsion

N	Failure modes
$10^3 \leq N \leq 10^4$	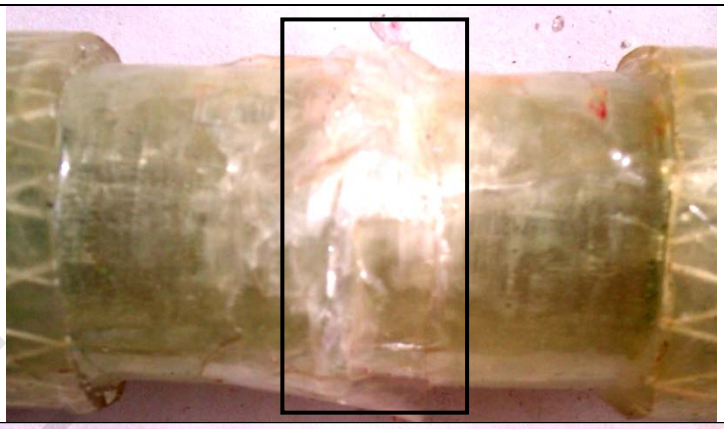
$10^4 \leq N \leq 10^5$	
$10^5 \leq N \leq 10^6$	

Table A2.6: The failure modes of M_2, $[0,90°]_{3s}$ specimens under completely reversed pure torsion

N	Failure modes
$10^3 \leq N \leq 10^4$	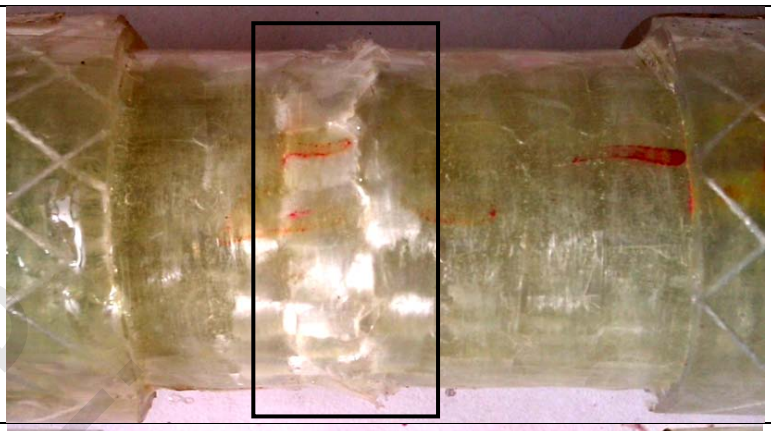
$10^4 \leq N \leq 10^5$	
$10^5 \leq N \leq 10^6$	

Table A2.7: The failure modes of M_1, $[\pm 45°]_{3s}$ specimens under completely reversed pure torsion

N	Failure modes
$10^3 \leq N \leq 10^4$	
$10^4 \leq N \leq 10^5$	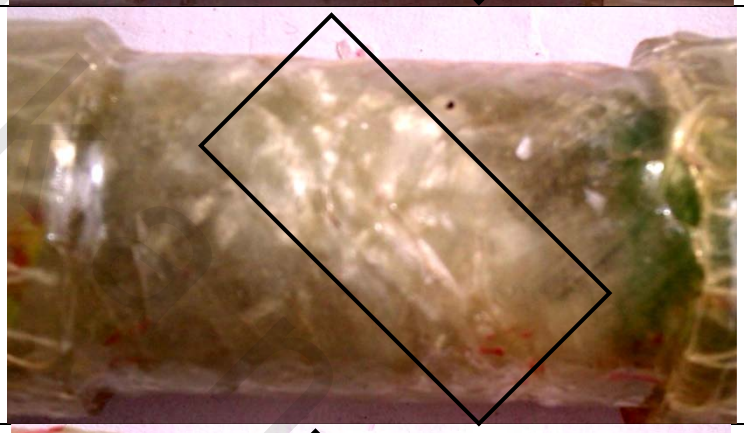
$10^5 \leq N \leq 10^6$	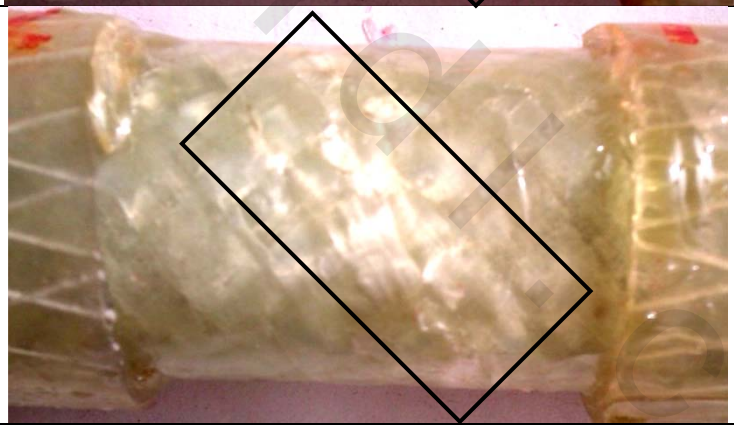

Table A2.8: The failure modes of M_2, $[\pm 45°]_{3s}$ under completely reversed pure torsion

N	Failure modes
$10^3 < N < 10^4$	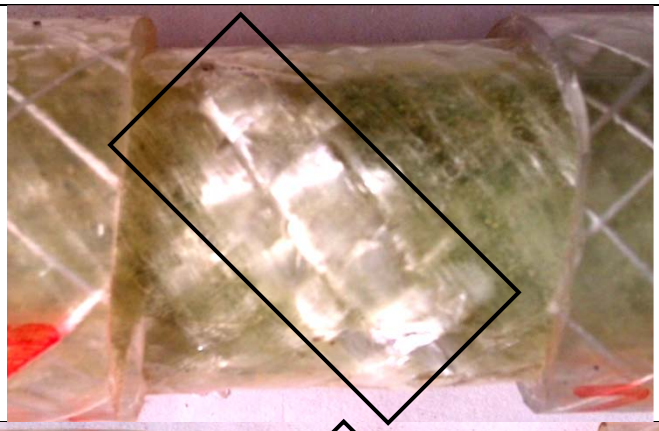
$10^4 < N < 10^5$	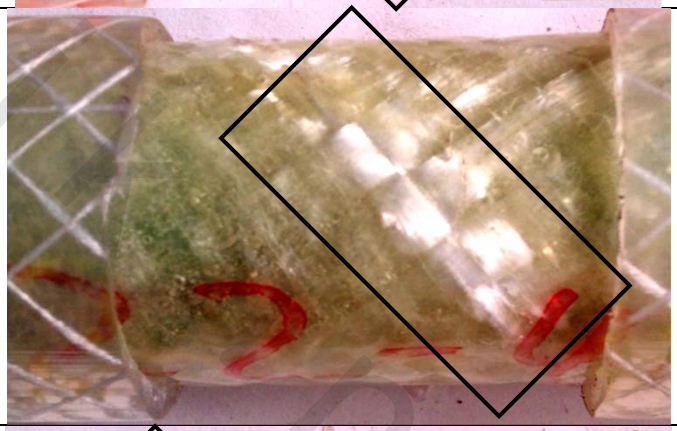
$10^5 < N < 10^6$	

A2.3 Completely Reversed Bending plus Static Internal Pressure Test

Table A2.9: The failure modes of M_1, $[0,90°]_{3s}$ specimens Under $P_r = 0.25$

N	Failure modes
$10^3 \leq N \leq 10^4$	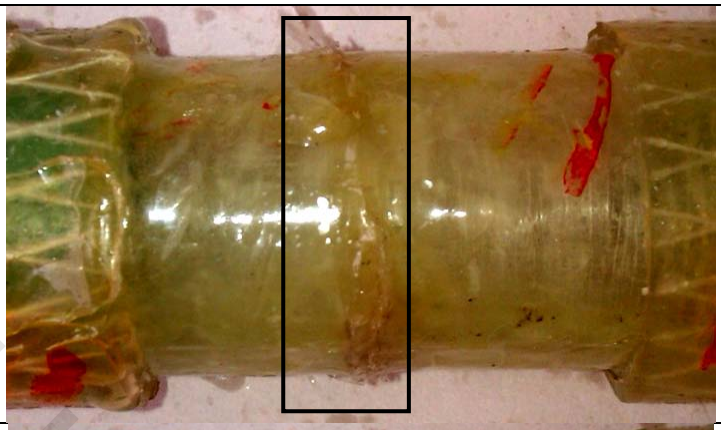
$10^4 \leq N \leq 10^5$	
$10^5 \leq N \leq 10^6$	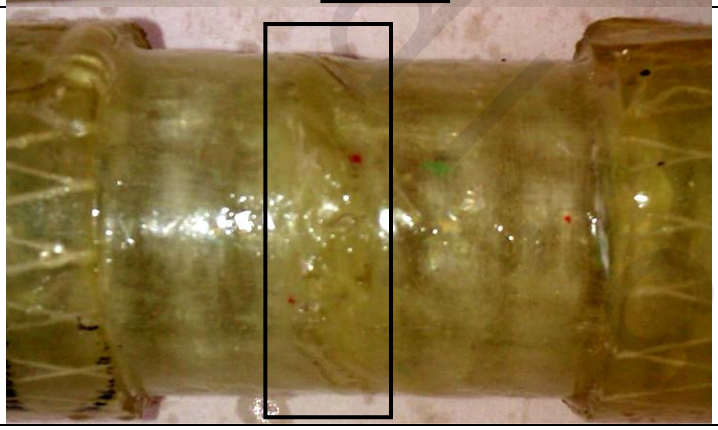

Table A2.10: The failure modes of M_2, $[0,90°]_{3s}$ specimens Under $P_r = 0.25$

N	Failure modes
$10^3 \leq N \leq 10^4$	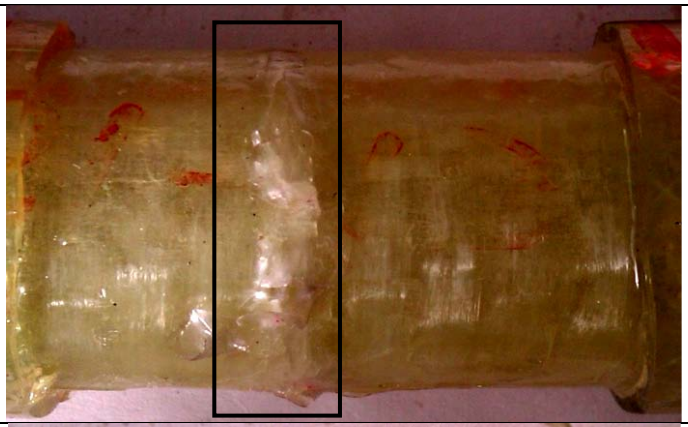
$10^4 \leq N \leq 10^5$	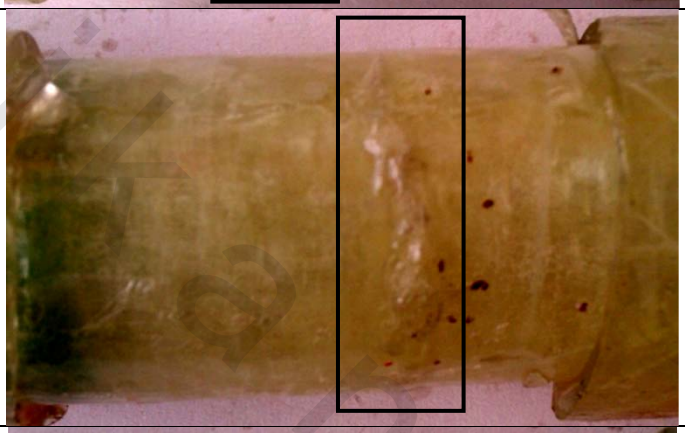
$10^5 \leq N \leq 10^6$	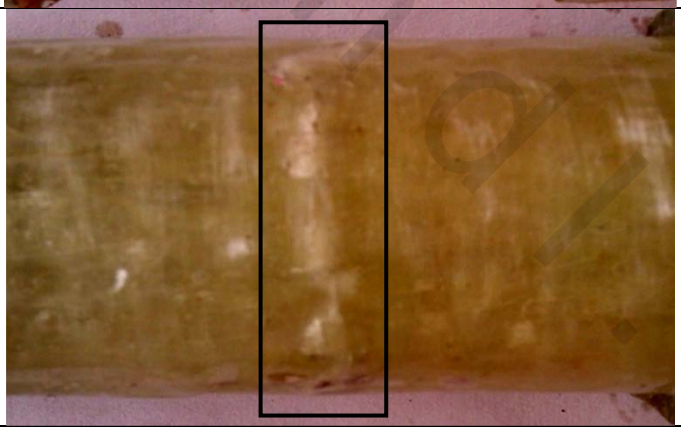

Table A2.11: The failure modes of M_1, $[\pm 45°]_{3s}$ specimens Under $P_r = 0.25$

N	Failure modes
$10^3 \leq N \leq 10^4$	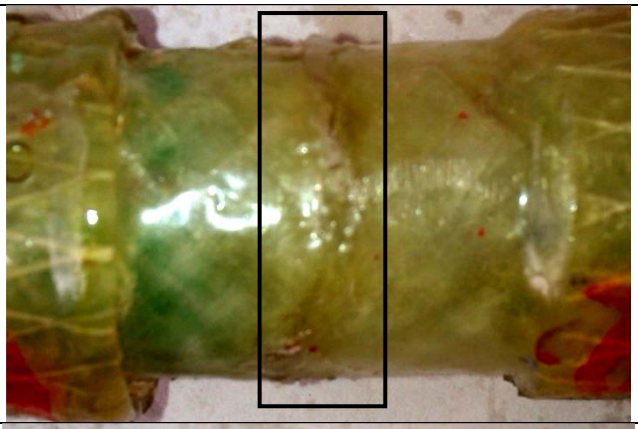
$10^4 \leq N \leq 10^5$	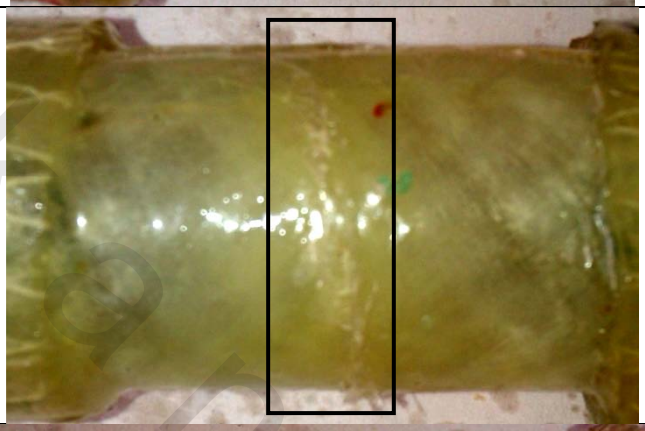
$10^5 \leq N \leq 10^6$	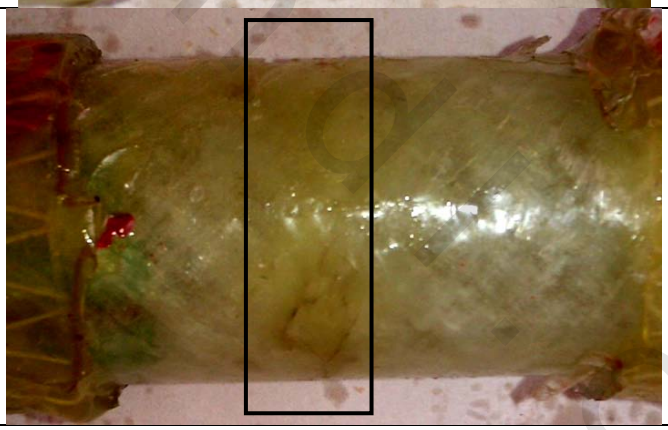

Table A2.12: The failure modes of M_2, $[\pm 45°]_{3s}$ specimens Under $P_r = 0.25$

N	Failure modes
$10^3 < N < 10^4$	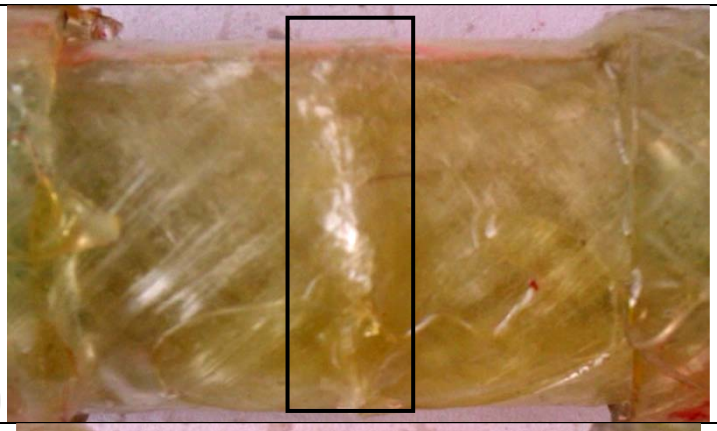
$10^4 < N < 10^5$	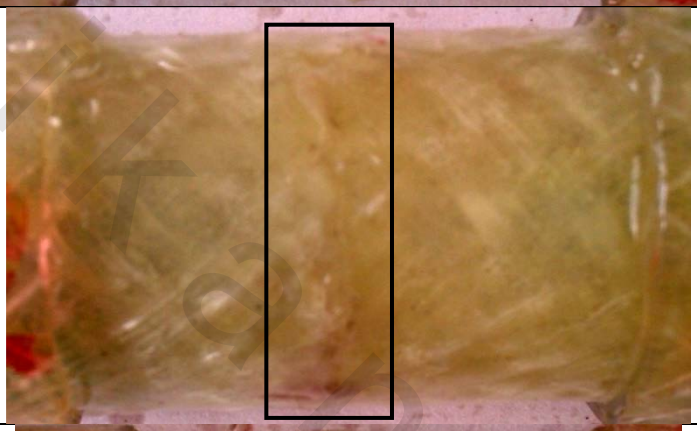
$10^5 < N < 10^6$	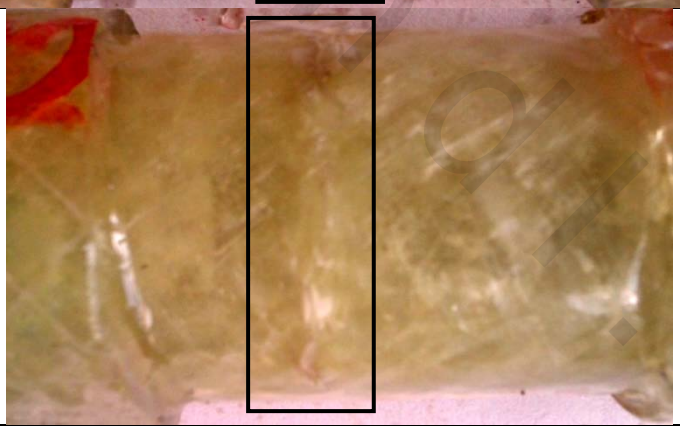

Table A2.13: The failure modes of M_1, $[0,90°]_{3s}$ specimens Under $P_r = 0.5$

N	Failure modes
$10^3 \leq N \leq 10^4$	
$10^4 \leq N \leq 10^5$	
$10^5 \leq N \leq 10^6$	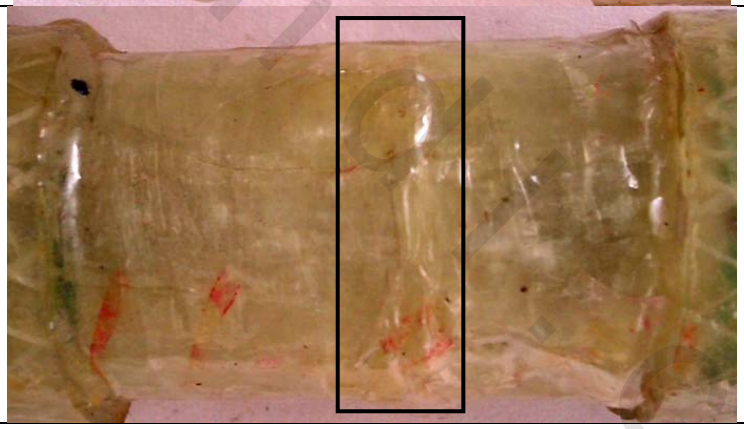

Table A2.14: The failure modes of M_2, $[0,90°]_{3s}$ specimens Under $P_r = 0.5$

N	Failure modes
$10^3 \leq N \leq 10^4$	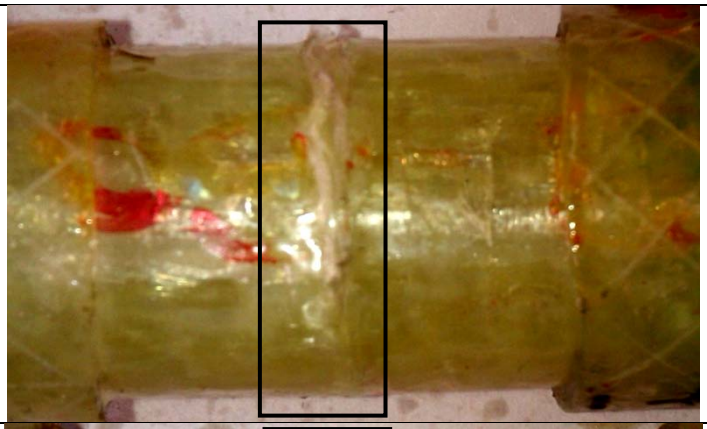
$10^4 \leq N \leq 10^5$	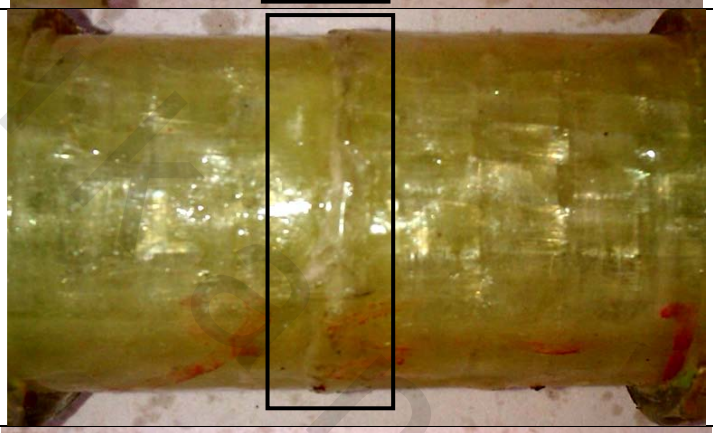
$10^5 \leq N \leq 10^6$	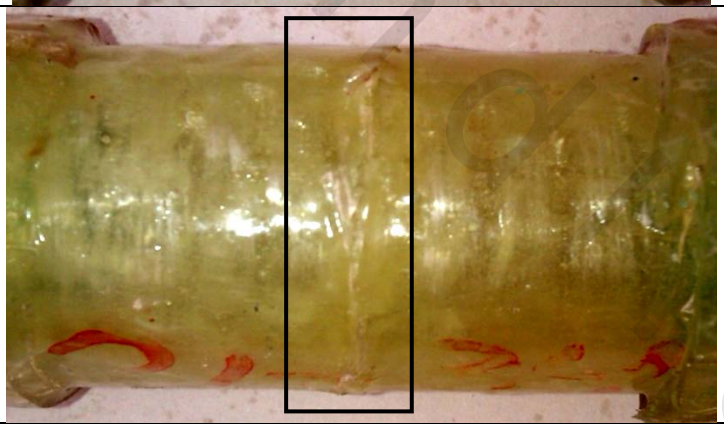

Table A2.15: The failure modes of M_1, $[\pm 45°]_{3s}$ specimens Under $P_r = 0.5$

N	Failure modes
$10^3 \leq N \leq 10^4$	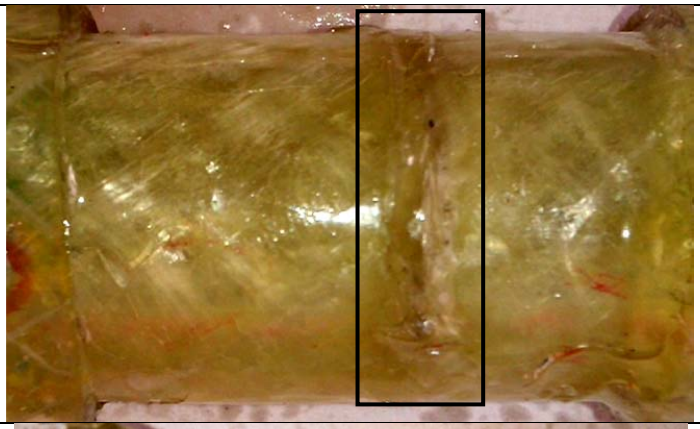
$10^4 \leq N \leq 10^5$	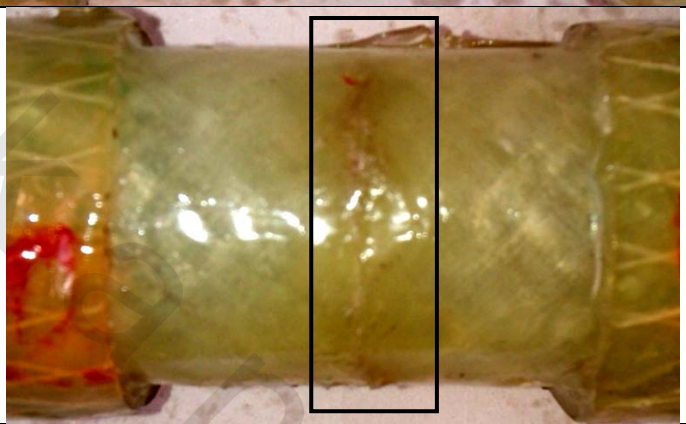
$10^5 \leq N \leq 10^6$	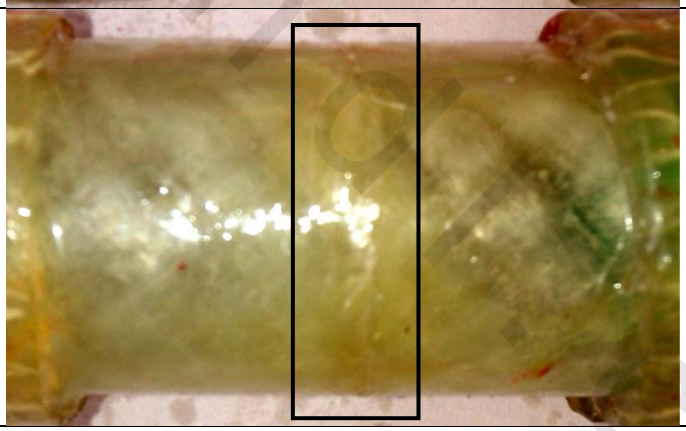

Table A2.16: The failure modes of M_2, $[\pm 45°]_{3s}$ specimens Under $P_r = 0.5$

N	Failure modes
$10^3 \leq N \leq 10^4$	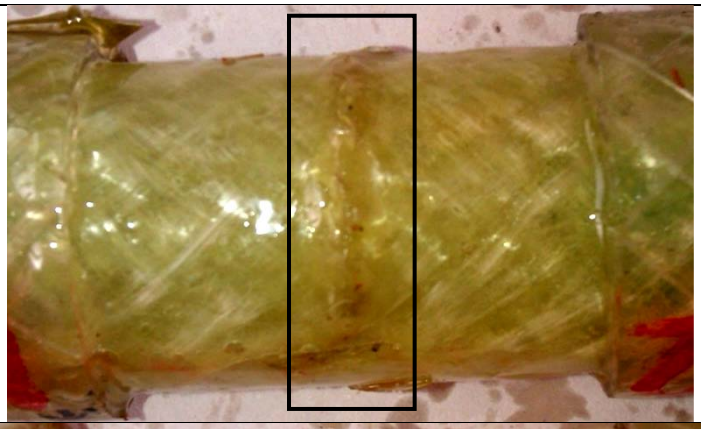
$10^4 \leq N \leq 10^5$	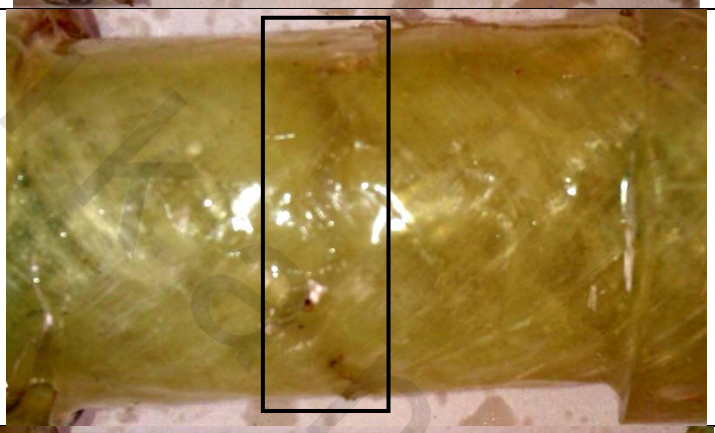
$10^5 \leq N \leq 10^6$	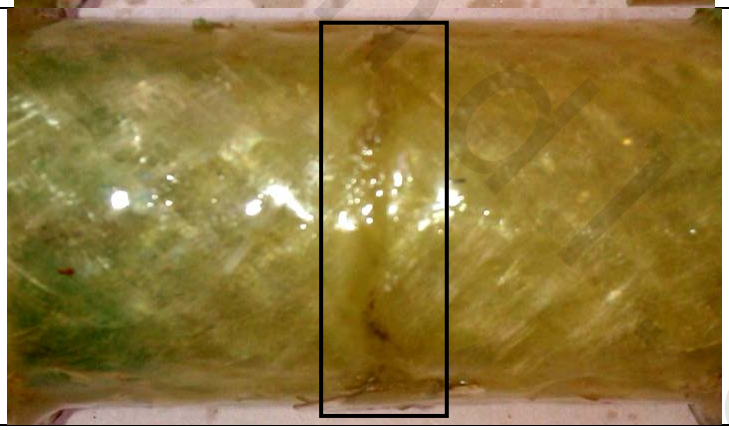

Table A2.17: The failure modes of M_1, $[0,90°]_{3s}$ specimens Under $P_r = 0.75$

N	Failure modes
$10^3 \leq N \leq 10^4$	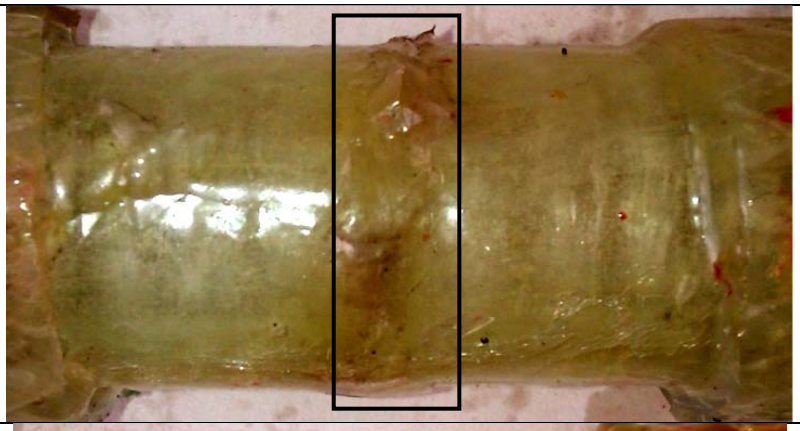
$10^4 \leq N \leq 10^5$	
$10^5 \leq N \leq 10^6$	

Table A2.18: The failure modes of M_2, $[0,90°]_{3s}$ specimens Under $P_r = 0.75$

N	Failure modes
$10^3 \leq N \leq 10^4$	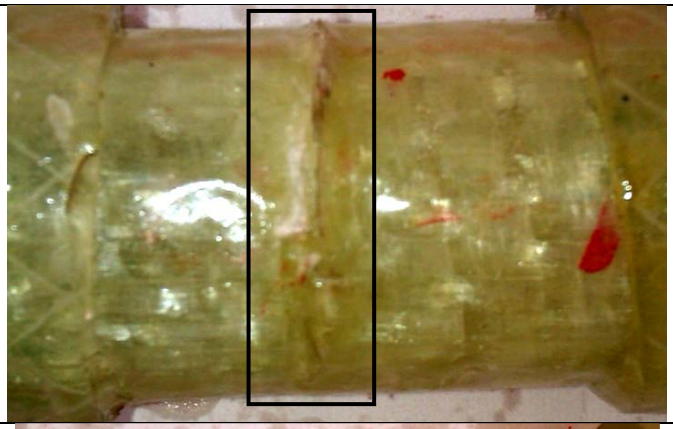
$10^4 \leq N \leq 10^5$	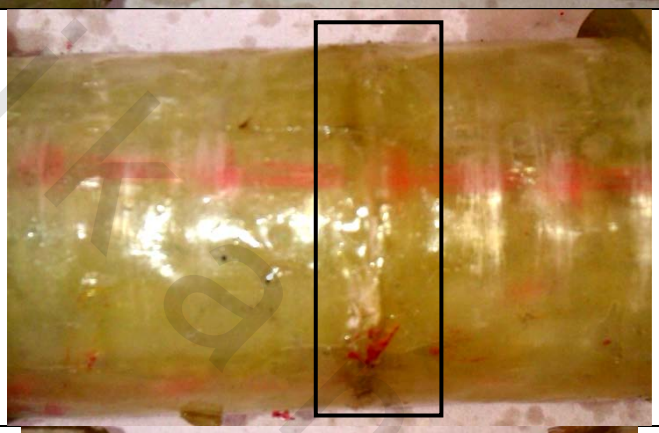
$10^5 \leq N \leq 10^6$	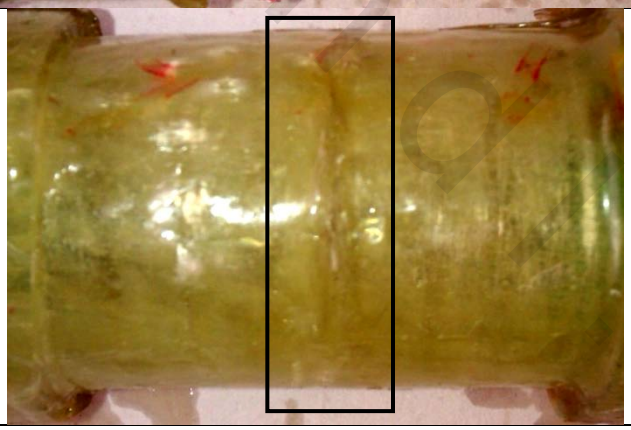

Table A2.19: The failure modes of M_1, $[\pm 45°]_{3s}$ specimens Under $P_r = 0.75$

N	Failure modes
$10^3 \leq N \leq 10^4$	
$10^4 \leq N \leq 10^5$	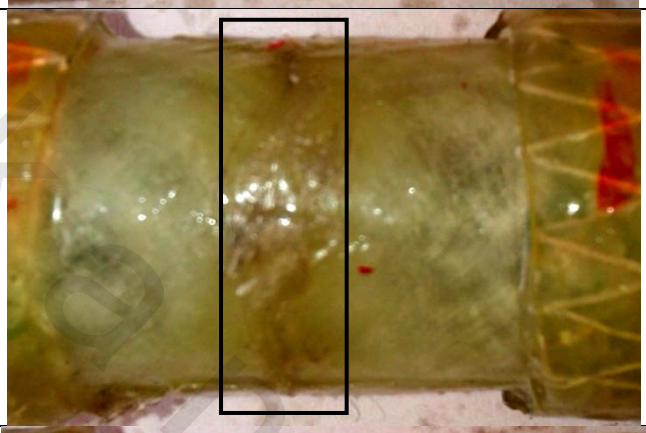
$10^5 \leq N \leq 10^6$	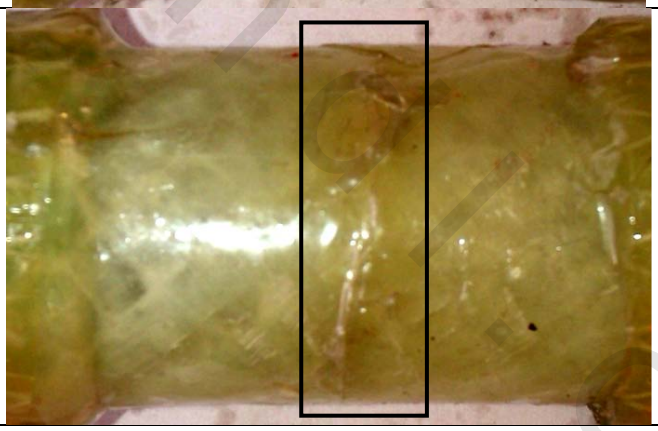

Table A2.20: The failure modes of M_2, $[\pm 45°]_{3s}$ specimens Under $P_r = 0.75$

N	Failure modes
$10^3 \leq N \leq 10^4$	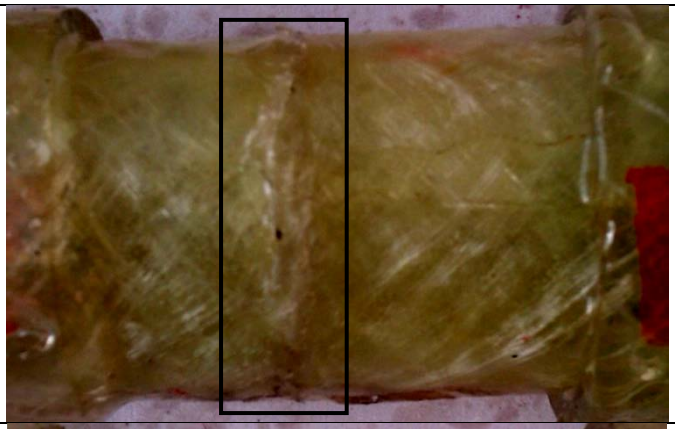
$10^4 \leq N \leq 10^5$	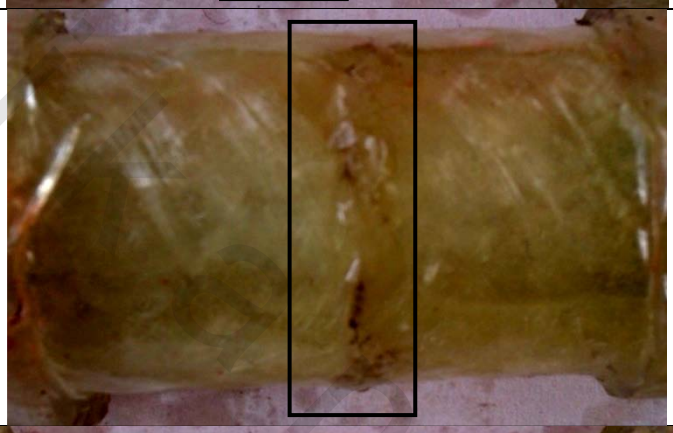
$10^5 \leq N \leq 10^6$	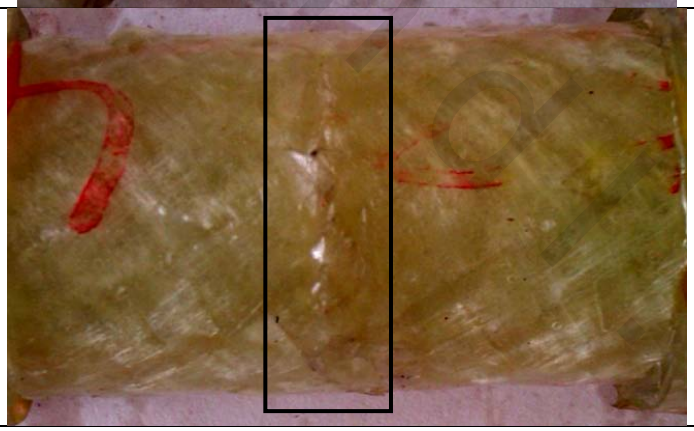

APPENDIX (3)

TABLES OF RESULTS AND CALIBRATION

A3.1 Material Properties

Table A3.1.Properties of used hydraulic oil **[164]**

Property	Value
Trade name	Mobil DTE 26
ISO Grade	68
SAE Grade	10
Kinematic Viscosity	71 (mm^2/sec) at 40C° 8.5 (mm^2/sec) at 100C°
Density	881 (Kg/m^3) at 15C°
Pour Point	-21C°
Flash Point	236C°
Solubility in Water	Negligible
Vapor Pressure	<0.013 kPa at 20C°
Auto ignition Temperature	N/D

Table A3.2.Properties of used materials **[84]**

Woven-roving E-glass fibers		**Epoxy Resin**	
Property	**Value**	**Property**	**Value**
Density	2551 kg/m^3	Density	1800 kg/m^3
Modulus of elasticity	E = 76 GPa	Modulus of elasticity	E = 3.6 GPa
Poisson's ratio	$\nu = 0.37$	Poisson's ratio	$\nu = 0.35$
Tensile strength	3.45 GPa	Tensile strength	0.25 GPa
Average mass/area	600 g/m^2	Gel time at 25°C	8 hour
Average thickness	0.69 mm	Full hardness time at 25°C	7 days
Weave	Plain	Percentage of mixing	2:1 by weights

A3.2 Calibration Bending Test

Table A3.3: The bending moment loading system specification

Calibration Part	Value
The length of bending moment loading arm Figure 4.3 (17).	675 mm
The length of intermediate shaft Figure 4.3 (8).	210 mm
The length of bending loading arm Figure 4.3 (4).	225 mm
The radius of intermediate shaft Figure 4.3 (8).	40 mm
The Time / Div	1 µ sec

Table A3.4: The bending moment loading system Calculation

I/P Volts (volts)	Gain of Amplifier	Volts/ Div (m volts)	Applied Mass (kg)	simulated bending (N.mm)
2.7	2	10.5	2.045	35546.4
			3.595	62488.6
			5.145	89431
			6.17	107247.5
			7.725	134276.7
			10.3	179035.6
			11.845	205891
			13.4	232920
			15.46	268727.2
			17	295495.6

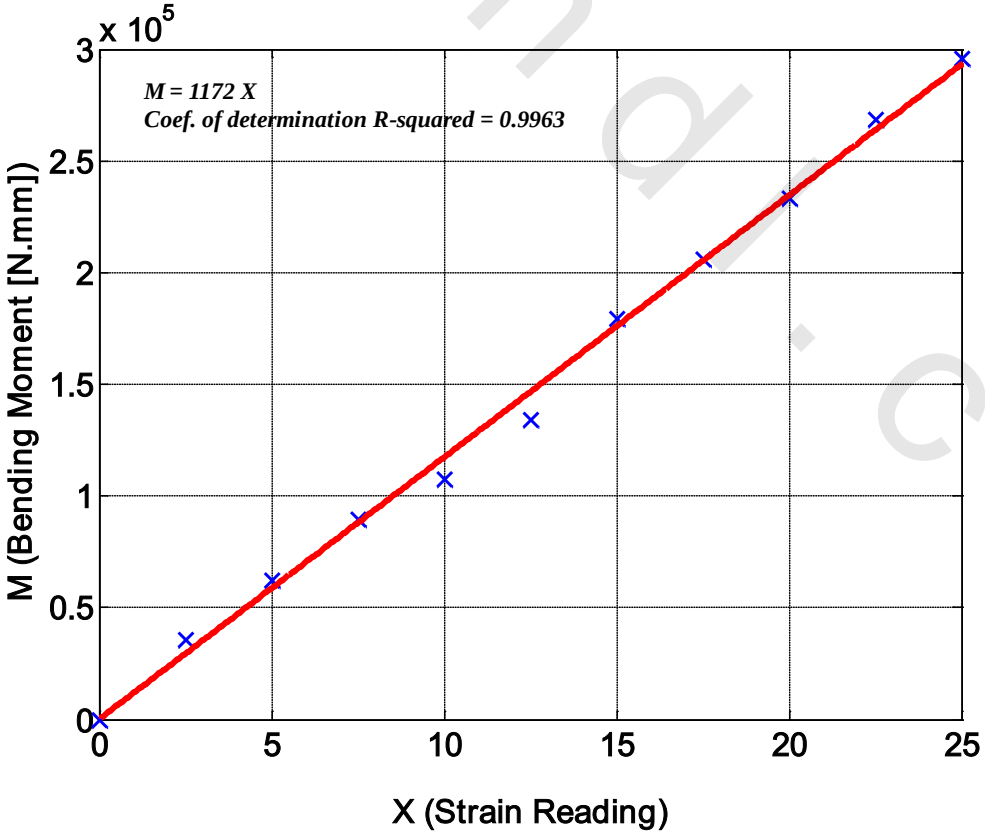

Figure A3.2.Calibration of Bending Arm (Gain Factor 2 and Volts/ Div 10.5 [(m volts])

A3.3 Calibration Torsion Test

Table A3.5: The torsion loading system specification

Calibration Part	Value
The length of Twisting moment loading arm Figure 4.3 (16).	765 mm
The radius of Guide shaft Figure 4.3 (10).	40 mm
The Time / Div	1 µ sec

Table A3.6: The torsion loading system Calculation

I/P Volts (volts)	Gain of Amplifier	Volts/ Div (m volts)	Applied Mass (kg)	simulated bending (N.mm)
4.35	0.31	10.5	4.65	30791.1
			9.18	60787.6
			13.96	92439.6
			19.095	126442.3
			23.13	153161

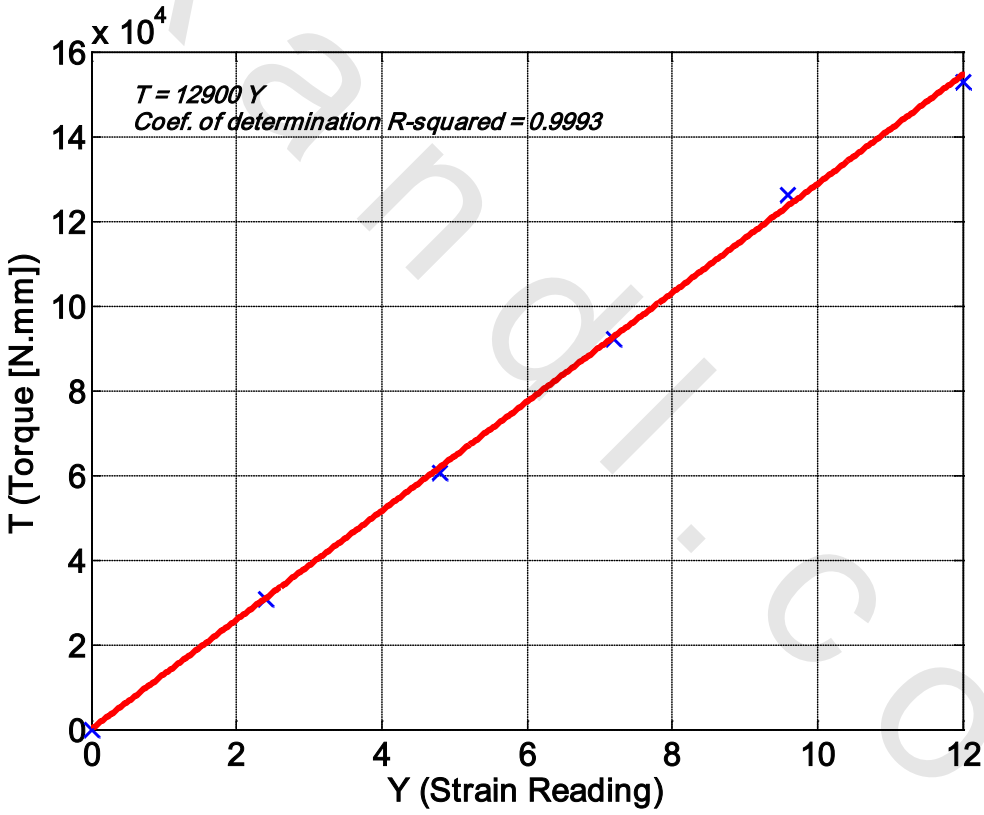

Figure A3.4.Calibration of Torsion Arm (Gain Factor 0.31 and Volts/ Div 10.5[(m volts])

A3.4 Static Bending and Torsion Test

Table A3.7: Static Bending Test Data of M_1, $[0,90°]_{3s}$

Specimen Code	d_o [mm]	d_i [mm]	Volume Fraction V_f	Ultimate bending Strength S_u (MPa)	Average Value (MPa)
WA041-M1A1T011	24.12	19.94	0.61	183.5	181.8 ≅ 182
WA042-M1A1T011	24.13	19.95	0.58	175.36	
WA043-M1A1T011	24.29	20.05	0.56	186.52	

Table A3.8: Static Bending Test Data of M_1, $[\pm45°]_{3s}$

Specimen Code	d_o [mm]	d_i [mm]	Volume Fraction V_f	Ultimate bending Strength S_u (MPa)	Average Value (MPa)
WA041-M1A2T011	24.3	20.08	*0.63*	163.6	159.1 ≅ 159
WA042-M1A2T011	24.03	19.75	*0.60*	158.15	
WA043-M1A2T011	24.17	19.87	*0.58*	155.54	

Table A3.9: Static Bending Test Data of M_2, $[0,90°]_{3s}$

Specimen Code	d_o [mm]	d_i [mm]	Volume Fraction V_f	Ultimate bending Strength S_u (MPa)	Average Value (MPa)
WA041-M2A1T011	26.07	20.23	*0.61*	206.16	197.65 ≅ 198
WA042-M2A1T011	26.84	20.48	*0.58*	196.2	
WA043-M2A1T011	26.64	20.3	*0.63*	190.57	

Table A3.10: Static Bending Test Data of M_2, $[\pm45°]_{3s}$

Specimen Code	d_o [mm]	d_i [mm]	Volume Fraction V_f	Ultimate bending Strength S_u (MPa)	Average Value (MPa)
WA041-M2A2T011	26.55	20.45	*0.64*	177.2	172.67 ≅ 173
WA042-M2A2T011	26.17	20.11	*0.58*	173.86	
WA043-M2A2T011	26.39	20.13	*0.63*	167	

Table A3.11: Static Torsion Test Data of M_1, $[0,90°]_{3s}$

Specimen Code	d_o [mm]	d_i [mm]	Volume Fraction V_f	Ultimate shear Strength S_{us} (MPa)	Average Value (MPa)
WA044-M1A1T012	24.03	19.85	*0.57*	70.8	69.41 ≅ 69.5
WA045-M1A1T012	24	19.76	*0.56*	65.87	
WA046-M1A1T012	24.03	19.91	*0.55*	71.56	

Table A3.12: Static Torsion Test Data of M_1, $[\pm 45°]_{3s}$

Specimen Code	d_o [mm]	d_i [mm]	Volume Fraction V_f	Ultimate shear Strength S_{us} (MPa)	Average Value (MPa)
WA044-M1A2T012	24.77	20.25	*0.58*	82	83.66 ≅ 84
WA045-M1A2T012	24.41	20.17	*0.58*	84.56	
WA046-M1A2T012	24.5	20.3	*0.56*	84.44	

Table A3.13: Static Torsion Test Data of M_2, $[0,90°]_{3s}$

Specimen Code	d_o [mm]	d_i [mm]	Volume Fraction V_f	Ultimate shear Strength S_{us} (MPa)	Average Value (MPa)
WA044-M2A1T012	26.22	20.16	*0.62*	22.34	23.758 ≅ 24
WA045-M2A1T012	26.34	20.16	*0.65*	21.83	
WA046-M2A1T012	26.29	19.99	*0.63*	27.1	

Table A3.14: Static Torsion Test Data of M_2, $[\pm 45°]_{3s}$

Specimen Code	d_o [mm]	d_i [mm]	Volume Fraction V_f	Ultimate shear Strength S_{us} (MPa)	Average Value (MPa)
WA044-M2A2T012	26.76	20.34	*0.62*	36	34.68 ≅ 35
WA045-M2A2T012	26.17	20.01	*0.63*	33.36	
WA046-M2A2T012	26.06	20.18	*0.63*	34.72	

A3.5 Static Pressure Test

Table A3.15: Static Pressure Test Data of Closed Cylinder, M_1, $[0,90°]_{3s}$

Specimens code	Loading Time (sec)	Effective length l_1 [mm]	d_o [mm]	d_i [mm]	Volume Fraction V_f	Maximum Pressure Recorded $P_{i_{max}}$ (bars)
WA001-M1A1T113	23	34.69	24.53	20.09	*0.56*	55
WA002-M1A1T113	19	39.65	24.48	20.32	*0.55*	53
WA003-M1A1T113	31	41.12	24.13	19.99	*0.61*	57

Table A3.16: Stress –Strain Data of Closed Cylinder, M_1, $[0,90°]_{3s}$

Specimens code	Average Pressure (bars)	Average Pressure rate (bars/sec)	$\sigma_{H_{max}}$ (MPa)	σ_r (MPa)	σ_l (MPa)
WA001-M1A1T113	55	2.4	27.91	5.5	11.21
WA002-M1A1T113		2.8	28.78	5.3	11.74
WA003-M1A1T113		1.84	30.64	5.7	12.47

Table A3.17: Static Pressure Test Data of Closed Cylinder, M_1, $[\pm45°]_{3s}$

Specimens code	Loading Time (sec)	Effective length l_1 [mm]	d_o [mm]	d_i [mm]	Volume Fraction V_f	Maximum Pressure Recorded $P_{i_{max}}$ (bars)
WA001-M1A2T113	26	36.69	24.25	19.99	*0.58*	68
WA002-M1A2T113	22	24.67	24.11	19.61	*0.56*	73
WA003-M1A2T113	25	35.32	24.72	20.34	*0.63*	68

Table A3.18: Stress –Strain Data of Closed Cylinder, M_1, $[\pm45°]_{3s}$

Specimens code	Average Pressure (bars)	Average Pressure rate (bars/sec)	$\sigma_{H_{max}}$ (MPa)	σ_r (MPa)	σ_l (MPa)
WA001-M1A2T113	69.667	2.62	35.64	6.8	14.42
WA002-M1A2T113		3.32	35.84	7.3	14.27
WA003-M1A2T113		2.72	35.31	6.8	14.25

Table A3.19: Static Pressure Test Data of Closed Cylinder, M_2, $[0,90°]_{3s}$

Specimens code	Loading Time (sec)	Effective length l_1 [mm]	d_o [mm]	d_i [mm]	Volume Fraction V_f	Maximum Pressure Recorded $P_{i_{max}}$ (bars)
WA001-M2A1T113	32	46.92	26.96	20.64	*0.59*	88
WA002-M2A1T113	36	43.96	26.28	19.98	*0.57*	95
WA003-M2A1T113	39	41.35	26.7	20.28	*0.61*	92

Table A3.20: Stress –Strain Data of Closed Cylinder, M_2, $[0,90°]_{3s}$

Specimens code	Average Pressure (bars)	Average Pressure rate (bars/sec)	$\sigma_{H_{max}}$ (MPa)	σ_r (MPa)	σ_l (MPa)
WA001-M2A1T113	91.667	2.75	33.72	8.8	12.46
WA002-M2A1T113		2.34	35.53	9.5	13.013
WA003-M2A1T113		2.36	34.29	9.2	12.55

Table A3.21: Interface Pressures Data of Closed Cylinder, M_2, $[0,90°]_{3s}$

Specimens code	P_{1-2} (Mpa)	P_{2-3} (Mpa)	E (Gpa)
WA001-M2A1T113	5.0441	2.2021	44.3862
WA002-M2A1T113	5.4213	2.3584	44.3862
WA003-M2A1T113	5.2469	2.2815	44.3862

Table A3.22: Static Pressure Test Data of Closed Cylinder, M_2, $[\pm45°]_{3s}$

Specimens code	Loading Time (sec)	Effective length l_1 [mm]	d_o [mm]	d_i [mm]	Volume Fraction V_f	Maximum Pressure Recorded $P_{i_{max}}$ (bars)
WA001-M2A2T113	37	41.61	26.41	20.37	*0.66*	108
WA002-M2A2T113	34	38.73	26.81	20.45	*0.69*	110
WA003-M2A2T113	33	42.88	26.48	20.48	*0.63*	118

Table A3.23: Stress –Strain Data of Closed Cylinder, M_2, $[\pm45°]_{3s}$

Specimens code	Average Pressure (bars)	Average Pressure rate (bars/sec)	$\sigma_{H_{max}}$ (MPa)	σ_r (MPa)	σ_l (MPa)
WA001-M2A2T113	112	2.92	42.52	10.8	15.86
WA002-M2A2T113		3.24	41.61	11	15.3
WA003-M2A2T113		3.6	46.93	11.8	17.57

Table A3.24: Interface Pressures Data of Closed Cylinder, M_2, $[\pm45°]_{3s}$

Specimens code	P_{1-2} (Mpa)	P_{2-3} (Mpa)	E (Gpa)
WA001-M2A2T113	6.2196	2.7257	24.2425
WA002-M2A2T113	6.2905	2.7411	24.2425
WA003-M2A2T113	6.8072	2.9874	24.2425

Table A3.25: Static Pressure Test Data of Open Cylinder, M_1, $[0,90°]_{3s}$

Specimens code	Loading Time (sec)	Effective length l_1 [mm]	d_o [mm]	d_i [mm]	Volume Fraction V_f	Maximum Pressure Recorded $P_{i_{max}}$ (bars)
WA004-M1A1T213	25	35.4	24.44	20.24	*0.59*	63
WA005-M1A1T213	27	33.6	24.32	20.08	*0.58*	67
WA006-M1A1T213	32	34	24.66	20.54	*0.56*	65

Table A3.26: Stress –Strain Data of Open Cylinder, M_1, $[0,90°]_{3s}$

Specimens code	Average Pressure (bars)	Average Pressure rate (bars/sec)	$\sigma_{H_{max}}$ (MPa)	σ_r (MPa)	σ_l (MPa)
WA004-M1A1T213	65	2.52	33.81	6.3	0
WA005-M1A1T213		2.48	35.4	6.7	0
WA006-M1A1T213		2.03	35.95	6.5	0

Table A3.27: Static Pressure Test Data of Open Cylinder, M_1, $[\pm45°]_{3s}$

Specimens code	Loading Time (sec)	Effective length l_1 [mm]	d_o [mm]	d_i [mm]	Volume Fraction V_f	Maximum Pressure Recorded $P_{i_{max}}$ (bars)
WA004-M1A2T213	31	29.27	24.5	20.26	*0.61*	75
WA005-M1A2T213	36	35	24.3	19.94	*0.60*	90
WA006-M1A2T213	33	35.5	24.21	20.05	*0.57*	87

Table A3.28: Stress –Strain Data of Open Cylinder, M_1, $[\pm45°]_{3s}$

Specimens code	Average Pressure (bars)	Average Pressure rate (bars/sec)	$\sigma_{H_{max}}$ (MPa)	σ_r (MPa)	σ_l (MPa)
WA004-M1A2T213	84	2.42	39.94	7.5	0
WA005-M1A2T213		2.5	46.1	9	0
WA006-M1A2T213		2.64	46.69	8.7	0

Table A3.29: Static Pressure Test Data of Open Cylinder, M_2, $[0,90°]_{3s}$

Specimens code	Loading Time (sec)	Effective length l_1 [mm]	d_o [mm]	d_i [mm]	Volume Fraction V_f	Maximum Pressure Recorded $P_{i_{max}}$ (bars)
WA004-M2A1T213	52	38.55	26.6	20.32	*0.59*	105
WA005-M2A1T213	56	49.49	26.79	20.57	*0.57*	115
WA006-M2A1T213	58	42.8	26.38	20.12	*0.65*	125

Table A3.30: Stress –Strain Data of Open Cylinder, M_2, $[0,90°]_{3s}$

Specimens code	Average Pressure (bars)	Average Pressure rate (bars/sec)	$\sigma_{H_{max}}$ (MPa)	σ_r (MPa)	σ_l (MPa)
WA004-M2A1T213	115	2.02	39.93	10.5	0
WA005-M2A1T213		2.05	44.54	11.5	0
WA006-M2A1T213		2.16	47.27	12.5	0

Table A3.31: Interface Pressures Data of Open Cylinder, M_2, $[0,90°]_{3s}$

Specimens code	P_{1-2} (Mpa)	P_{2-3} (Mpa)	E (Gpa)
WA004-M2A1T213	6.0102	2.621	44.3862
WA005-M2A1T213	6.6039	2.8875	44.3862
WA006-M2A1T213	7.1478	3.1146	44.3862

Table A3.32: Static Pressure Test Data of Open Cylinder, M_2, $[\pm 45°]_{3s}$

Specimens code	Loading Time (sec)	Effective length l_1 [mm]	d_o [mm]	d_i [mm]	Volume Fraction V_f	Maximum Pressure Recorded $P_{i_{max}}$ (bars)
WA004-M2A2T213	66	38.56	26.13	20.07	*0.68*	150
WA005-M2A2T213	73	39.43	26.39	20.47	*0.59*	153
WA006-M2A2T213	77	39.22	26.7	20.42	*0.60*	158

Table A3.33: Stress –Strain Data of Open Cylinder, M_2, $[\pm 45°]_{3s}$

Specimens code	Average Pressure (bars)	Average Pressure rate (bars/sec)	$\sigma_{H_{max}}$ (MPa)	σ_r (MPa)	σ_l (MPa)
WA004-M2A2T213	153.667	2.27	58.16	15	0
WA005-M2A2T213		2.1	61.52	15.3	0
WA006-M2A2T213		2.05	60.33	15.8	0

Table A3.34: Interface Pressures Data of Open Cylinder, M_2, $[\pm 45°]_{3s}$

Specimens code	P_{1-2} (Mpa)	P_{2-3} (Mpa)	E (Gpa)
WA004-M2A2T213	8.6157	3.7677	24.2425
WA005-M2A2T213	8.8425	3.8864	24.2425
WA006-M2A2T213	9.0506	3.9492	24.2425

A3.6 Completely Reversed Pure Bending Test

Table A3.35: Completely Reversed Pure Bending specimens Data of M_1, $[0,90°]_{3s}$ with $P_r = 0$

Specimens code	d_o [mm]	d_i [mm]	Volume Fraction V_f	σ_{max}(MPa)	Cycles to Failure (N)
WA019-M1A1T021	24.32	20.16	0.59	109.9286	2135
WA021-M1A1T021	24.13	19.81	0.61	101.0584	4715
WA023-M1A1T021	24.06	19.84	0.60	95.4995	7385
WA022-M1A1T021	24.07	19.99	0.61	89.6371	16165
WA018-M1A1T021	24.55	20.05	0.60	72.5155	37065
WA017-M1A1T021	24.07	19.79	0.59	70.7612	55015
WA024-M1A1T021	24.25	20.15	0.61	63.8016	110565
WA020-M1A1T021	24.08	19.92	0.60	48.036	1000000

Table A3.36: Completely Reversed Pure Bending specimens Data of M_1, $[\pm 45°]_{3s}$ with $P_r = 0$

Specimens code	d_o [mm]	d_i [mm]	Volume Fraction V_f	σ_{max}(MPa)	Cycles to Failure (N)
WA018-M1A2T021	24.26	19.82	0.61	82.7775	3035
WA021-M1A2T021	24.43	19.89	0.63	72.8669	5615
WA024-M1A2T021	24.7	20.26	0.62	68.5909	8885
WA022-M1A2T021	24.16	19.82	0.63	65.5849	17665
WA019-M1A2T021	24.39	20.05	0.62	60.3974	38565
WA023-M1A2T021	24.18	19.92	0.61	54.6008	64015
WA020-M1A2T021	24.22	19.86	0.63	49.6478	119565
WA017-M1A2T021	24.23	19.93	0.62	38.4843	1000000

Table A3.37: Completely Reversed Pure Bending specimens specification of M_2, $[0,90°]_{3s}$ with $P_r = 0$

Specimens code	d_o [mm]	d_i [mm]	Volume Fraction V_f	σ_{max}(MPa)	Cycles to Failure (N)
WA021-M2A1T021	26.12	19.82	0.60	142.2521	2125
WA018-M2A1T021	26.87	20.43	0.64	122.8745	4085
WA023-M2A1T021	26.37	20.23	0.59	121.5163	6755
WA020-M2A1T021	26.7	20.48	0.63	98.2668	16730
WA019-M2A1T021	26.59	20.29	0.59	88.7846	37630
WA017-M2A1T021	26.55	20.49	0.62	81.1128	65725
WA022-M2A1T021	26.43	20.67	0.59	73.883	121275
WA024-M2A1T021	26.09	19.93	0.67	52.652	1000000

Table A3.38: Completely Reversed Pure Bending specimens Data of M_2, $[\pm 45°]_{3s}$ with $P_r = 0$

Specimens code	d_o [mm]	d_i [mm]	Volume Fraction V_f	σ_{max}(MPa)	Cycles to Failure (N)
WA023-M2A2T021	26.49	19.99	0.57	126.0169	2905
WA020-M2A2T021	26.09	20.01	0.62	109.5843	5285
WA019-M2A2T021	26.16	19.96	0.59	97.6666	10450
WA017-M2A2T021	26.28	20.24	0.60	88.0248	19230
WA018-M2A2T021	26.22	20.14	0.59	77.9401	42330
WA022-M2A2T021	26.23	19.81	0.66	65.8279	98280
WA024-M2A2T021	26.29	20.41	0.61	58.3144	251225
WA021-M2A2T021	26.19	20.13	0.59	47.6032	1000000

A3.7 Completely Reversed Pure Torsion Test

Table A3.39: Completely Reversed Pure Torsion specimens Data of M_1, $[0,90°]_{3s}$

Specimens code	d_o [mm]	d_i [mm]	Volume Fraction V_f	τ_{max}(MPa)	Cycles to Failure (N)
WA049-M1A1T022	24.12	19.94	0.60	37.24	739
WA051-M1A1T022	24.13	19.95	0.59	35	1236
WA053-M1A1T022	24.29	20.05	0.59	31.988	1985
WA052-M1A1T022	24.03	19.85	0.61	30.9	3281
WA048-M1A1T022	24.43	20.19	0.59	25.235	12210
WA047-M1A1T022	24.17	20.07	0.60	22.1	31927
WA054-M1A1T022	24	19.76	0.60	17.47	112164
WA050-M1A1T022	24.03	19.91	0.60	13.3126	1000000

Table A3.40: Completely Reversed Pure Torsion specimens Data of M_1, $[\pm 45°]_{3s}$

Specimens code	d_o [mm]	d_i [mm]	Volume Fraction V_f	τ_{max}(MPa)	Cycles to Failure (N)
WA048-M1A2T022	24.49	20.09	0.62	53.1	1364
WA051-M1A2T022	24.3	20.08	0.61	51.38	2579
WA054-M1A2T022	24.03	19.75	0.61	47.81	4372
WA052-M1A2T022	24.17	19.87	0.63	42.73	9188
WA049-M1A2T022	24.77	20.25	0.61	35.1	76150
WA053-M1A2T022	24.41	20.17	0.62	33.75	90107
WA050-M1A2T022	24.5	20.3	0.63	29.47	325572
WA047-M1A2T022	24.31	20.17	0.62	25.97	1000000

Table A3.41: Completely Reversed Pure Torsion specimens Data of M_2, $[0,90°]_{3s}$

Specimens code	d_o [mm]	d_i [mm]	Volume Fraction V_f	τ_{max}(MPa)	Cycles to Failure (N)
WA051-M2A1T022	26.07	20.23	0.67	14.47	380
WA048-M2A1T022	26.32	20.12	0.59	12.25	614
WA053-M2A1T022	26.84	20.48	0.58	10.21	1187
WA050-M2A1T022	26.64	20.3	0.665	9.1	1983
WA049-M2A1T022	26.22	20.16	0.59	8.33	5106
WA047-M2A1T022	26.45	20.27	0.59	5.34	50033
WA052-M2A1T022	26.34	20.16	0.58	4.03	102463
WA054-M2A1T022	26.29	19.99	0.58	2.64	1000000

Table A3.42: Completely Reversed Pure Torsion specimens Data of M_2, $[\pm 45°]_{3s}$

Specimens code	d_o [mm]	d_i [mm]	Volume Fraction V_f	τ_{max}(MPa)	Cycles to Failure (N)
WA053-M2A2T022	26.55	20.45	0.65	21.61	674
WA050-M2A2T022	26.17	20.11	0.58	19.63	1027
WA049-M2A2T022	26.39	20.13	0.58	17.5	1992
WA047-M2A2T022	26.4	20.04	0.61	15.97	2995
WA048-M2A2T022	26.55	20.23	0.58	13.17	7711
WA052-M2A2T022	26.76	20.34	0.59	10.22	55561
WA054-M2A2T022	26.17	20.01	0.61	8.28	154743
WA051-M2A2T022	26.06	20.18	0.60	5.72	1000000

A3.8 Completely Reversed Bending plus Static Internal Pressure Test

Table A3.43: Data of M_1, $[0,90°]_{3s}$ with $P_r = 0.25$

Specimens code	d_o [mm]	d_i [mm]	Volume Fraction V_f	σ_l [MPa]	$\sigma_{H_{max}}$ [MPa]	σ_{max} [MPa]	Cycles to Failure (N)
WA025-M1A1T124	24.12	19.88	0.59	2.9128	6.8552	87.17338	1649
WA026-M1A1T124	24.47	20.03	0.56	2.792	6.9591	80.13931	3640
WA08-M1A1T124	24.08	19.98	0.57	3.0385	6.9244	75.7311	5702
WA028-M1A1T124	24.1	20.02	0.60	3.0615	6.9521	71.08222	12480
WA011-M1A1T124	24.36	20.14	0.61	2.97	7.0357	57.50479	28615
WA015-M1A1T124	24.46	20.18	0.61	2.9307	7.0637	56.11363	42472
WA030-M1A1T124	24.22	19.98	0.60	2.9289	6.9244	50.59467	85357
WA036-M1A1T124	24.36	20.08	0.55	2.9148	6.9939	38.09255	1000000

Table A3.44: Data of M_1, $[\pm45°]_{3s}$ with $P_r = 0.25$

Specimens code	d_o [mm]	d_i [mm]	Volume Fraction V_f	σ_l [MPa]	$\sigma_{H_{max}}$ [MPa]	σ_{max} [MPa]	Cycles to Failure (N)
WA010-M1A2T124	24.23	20.11	0.61	3.8741	8.7154	64.48367	2556
WA012-M1A2T124	24.7	20.18	0.57	3.5131	8.7762	56.76332	4728
WA015-M1A1T124	24.44	19.94	0.59	3.4841	8.5687	53.43231	7482
WA016-M1A2T124	24.28	20	0.62	3.6936	8.6203	51.09064	14874
WA029-M1A2T124	24.44	19.92	0.63	3.4633	8.5515	47.04957	32472
WA030-M1A2T124	24.33	19.89	0.63	3.5262	8.5258	42.53402	53901
WA031-M1A2T124	24.57	20.47	0.62	3.9709	9.0302	38.67564	100674
WA032-M1A2T124	24.37	20.05	0.56	3.6661	8.6635	29.97927	1000000

Table A3.45: Data of M_2, $[0,90°]_{3s}$ with $P_r = 0.25$

Specimens code	d_o [mm]	d_i [mm]	Volume Fraction V_f	σ_l [MPa]	$\sigma_{H_{max}}$ [MPa]	σ_{max} [MPa]	Cycles to Failure (N)
WA025-M2A1T124	26.77	20.57	0.60	3.3157	8.7235	109.8613	1477
WA07-M2A1T124	26.41	20.59	0.60	3.5647	8.7405	94.89598	2840
WA08-M2A1T124	26.49	19.97	0.66	3.028	8.222	93.84704	4695
WA028-M2A1T124	26.72	20.16	0.61	3.0396	8.3792	75.89145	11628
WA029-M2A1T124	26.43	20.35	0.64	3.3488	8.5379	68.56835	26153
WA011-M2A1T124	26.85	20.53	0.59	3.2374	8.6896	62.64342	45679
WA031-M2A1T124	26.07	20.39	0.59	3.6236	8.5715	57.05984	84287
WA013-M2A1T124	26.23	20.37	0.62	3.4948	8.5547	40.66314	1000000

Table A3.46: Data of M_2, $[\pm 45°]_{3s}$ with $P_r = 0.25$

Specimens code	d_o [mm]	d_i [mm]	Volume Fraction V_f	σ_l [MPa]	$\sigma_{H_{max}}$ [MPa]	σ_{max} [MPa]	Cycles to Failure (N)
WA07-M2A2T124	26.73	20.39	0.58	3.8967	10.5535	86.32158	2534
WA08-M2A1T124	26.53	20.31	0.62	3.9643	10.4709	75.06525	4609
WA027-M2A2T124	26.22	19.86	0.58	3.7683	10.012	66.90162	9113
WA010-M2A2T124	26.77	20.41	0.58	3.8871	10.5743	60.29699	16769
WA029-M2A2T124	26.35	20.05	0.62	3.8506	10.2045	53.38897	36912
WA013-M2A2T124	26.15	20.19	0.61	4.1326	10.3475	45.09211	85701
WA014-M2A2T124	26.51	20.09	0.59	3.7774	10.2453	39.94536	219069
WA032-M2A2T124	26.42	20.26	0.57	3.9969	10.4194	32.60819	1000000

Table A3.47: Data of M_1, $[0,90°]_{3s}$ with $P_r = 0.5$

Specimens code	d_o [mm]	d_i [mm]	Volume Fraction V_f	σ_l [MPa]	$\sigma_{H_{max}}$ [MPa]	σ_{max} [MPa]	Cycles to Failure (N)
WA033-M1A1T224	24.11	19.81	0.64	5.7144	14.1788	62.54937	1235
WA034-M1A1T224	24.06	19.86	0.62	5.88	14.2505	57.50223	2726
WA07-M1A1T224	24.33	20.21	0.56	6.1209	14.7572	54.33922	4269
WA010-M1A1T224	24.25	20.07	0.55	5.9793	14.5534	51.00351	9344
WA037-M1A1T224	24.14	19.96	0.56	5.9435	14.3943	41.26132	21424
WA038-M1A1T224	24.41	20.21	0.55	5.9936	14.7572	40.26312	31799
WA012-M1A1T224	24.11	19.91	0.59	5.8962	14.3223	36.30311	63907
WA040-M1A1T224	24.13	19.89	0.59	5.8289	14.2936	27.33248	1000000

Table A3.48: Data of M_1, $[\pm 45°]_{3s}$ with $P_r = 0.5$

Specimens code	d_o [mm]	d_i [mm]	Volume Fraction V_f	σ_l [MPa]	$\sigma_{H_{max}}$ [MPa]	σ_{max} [MPa]	Cycles to Failure (N)
WA033-M1A2T224	24.39	19.51	0.61	6.2187	15.9374	44.86541	1676
WA034-M1A2T224	24.77	20.35	0.65	7.2678	17.3393	39.49386	3100
WA011-M1A2T224	24.67	20.25	0.57	7.2286	17.1693	37.17627	4905
WA036-M1A2T224	24.14	19.82	0.57	7.2399	16.4479	35.54702	9752
WA013-M1A2T224	24.89	20.39	0.57	7.1414	17.4075	32.73539	21288
WA038-M1A2T224	24.49	20.09	0.56	7.2017	16.899	29.59363	35337
WA039-M1A2T224	24.42	20.04	0.61	7.2181	16.815	26.90911	66000
WA040-M1A2T224	24.42	20.08	0.61	7.3071	16.8822	20.85849	1000000

Table A3.49: Data of M_2, $[0,90°]_{3s}$ with $P_r = 0.5$

Specimens code	d_o [mm]	d_i [mm]	Volume Fraction V_f	σ_l [MPa]	$\sigma_{H_{max}}$ [MPa]	σ_{max} [MPa]	Cycles to Failure (N)
WA09-M2A1T224	26.15	19.83	0.61	6.2247	16.3097	78.52316	1129
WA016-M2A1T224	26.54	20.02	0.56	6.0733	16.6237	67.82672	2170
WA012-M2A1T224	26.32	20.42	0.62	6.9555	17.2946	67.077	3587
WA035-M2A1T224	26.58	20.26	0.67	6.3783	17.0246	54.24327	8884
WA014-M2A1T224	26.69	20.19	0.61	6.1536	16.9072	49.0091	19982
WA038-M2A1T224	26.01	20.29	0.68	7.1506	17.0751	44.77427	34900
WA039-M2A1T224	26.66	20.28	0.58	6.3173	17.0583	40.78342	64398
WA015-M2A1T224	26.24	19.84	0.57	6.1397	16.3261	29.0639	1000000

Table A3.50: Data of M_2, $[\pm 45°]_{3s}$ with $P_r = 0.5$

Specimens code	d_o [mm]	d_i [mm]	Volume Fraction V_f	σ_l [MPa]	$\sigma_{H_{max}}$ [MPa]	σ_{max} [MPa]	Cycles to Failure (N)
WA034-M2A2T224	26.25	20.23	0.695	8.1906	20.609	59.85803	1662
WA09-M2A2T224	26.4	20.38	0.67	8.2592	20.9158	52.05254	3024
WA011-M2A2T224	26.19	20.21	0.58	8.2433	20.5683	46.39164	5978
WA036-M2A2T224	26.17	20.13	0.60	8.1144	20.4058	41.81178	11000
WA037-M2A2T224	26.81	20.37	0.62	7.6476	20.8952	37.02155	24213
WA038-M2A2T224	26.15	19.87	0.59	7.6503	19.882	31.26825	56217
WA015-M2A2T224	26.65	20.49	0.60	8.0966	21.1422	27.69934	143701
WA016-M2A2T224	26.75	20.41	0.60	7.8021	20.9774	22.61152	1000000

Table A3.51: Data of M_1, $[0,90°]_{3s}$ with $P_r = 0.75$

Specimens code	d_o [mm]	d_i [mm]	Volume Fraction V_f	σ_l [MPa]	$\sigma_{H_{max}}$ [MPa]	σ_{max} [MPa]	Cycles to Failure (N)
WA055-M1A1T224	24.09	19.93	0.58	8.9474	20.4751	40.3438	966
WA056-M1A1T224	24.61	20.31	0.60	8.8092	21.2633	37.08843	2132
WA057-M1A1T224	24.1	19.98	0.59	9.0673	20.578	35.04832	3339
WA058-M1A1T224	24.18	19.92	0.59	8.7127	20.4545	32.89682	7307
WA059-M1A1T224	24.19	19.93	0.56	8.7175	20.4751	26.61319	16754
WA060-M1A1T224	24.3	20.14	0.61	9.0506	20.9089	25.96936	24867
WA061-M1A1T224	24.64	20.2	0.60	8.4543	21.0336	23.41519	49976
WA062-M1A1T224	24.36	20.08	0.59	8.7445	20.7845	17.62921	1000000

Table A3.52: Data of M_1, $[\pm 45°]_{3s}$ with $P_r = 0.75$

Specimens code	d_o [mm]	d_i [mm]	Volume Fraction V_f	σ_l [MPa]	$\sigma_{H_{max}}$ [MPa]	σ_{max} [MPa]	Cycles to Failure (N)
WA055-M1A2T224	24.69	20.53	0.60	11.7629	25.7603	27.81324	1199
WA056-M1A2T224	24.78	19.86	0.62	9.4282	24.1064	24.48328	2218
WA057-M1A2T224	24.53	20.25	0.61	11.2326	25.0625	23.04654	3510
WA058-M1A2T224	24.27	20.01	0.61	11.1439	24.4719	22.03653	6978
WA059-M1A2T224	24.72	20.08	0.62	10.1834	24.6434	20.29353	15234
WA060-M1A2T224	24.59	20.25	0.58	11.0625	25.0625	18.34587	25286
WA061-M1A2T224	24.49	20.09	0.57	10.8026	24.668	16.68166	47229
WA062-M1A2T224	24.42	20.04	0.61	10.8271	24.5453	12.93072	1000000

Table A3.53: Data of M_2, $[0,90°]_{3s}$ with $P_r = 0.75$

Specimens code	d_o [mm]	d_i [mm]	Volume Fraction V_f	σ_l [MPa]	$\sigma_{H_{max}}$ [MPa]	σ_{max} [MPa]	Cycles to Failure (N)
WA55-M2A1T224	26.79	20.63	0.57	10.0532	25.5663	53.48679	995
WA056-M2A1T224	26.37	20.39	0.645	10.2591	24.9749	46.20081	1912
WA057-M2A1T224	26.78	20.12	0.60	8.9425	24.3179	45.69013	3162
WA058-M2A1T224	26.27	20.43	0.59	10.5598	25.073	36.94832	7830
WA059-M2A1T224	26.25	20.01	0.62	9.5709	24.0527	33.38301	17611
WA060-M2A1T224	26.87	19.99	0.59	8.5523	24.0046	30.49841	30760
WA061-M2A1T224	26.23	20.19	0.57	10.0318	24.4874	27.78001	56757
WA062-M2A1T224	26.07	20.23	0.61	10.4435	24.5845	19.79715	1000000

Table A3.54: Data of M_2, $[\pm 45°]_{3s}$ with $P_r = 0.75$

Specimens code	d_o [mm]	d_i [mm]	Volume Fraction V_f	σ_l [MPa]	$\sigma_{H_{max}}$ [MPa]	σ_{max} [MPa]	Cycles to Failure (N)
WA055-M2A2T224	26.72	20.36	0.58	11.629	31.6579	36.79693	1267
WA056-M2A2T224	26.61	20.27	0.62	11.6121	31.3787	31.99862	2305
WA057-M2A2T224	26.77	20.57	0.58	12.1095	32.3144	28.51865	4557
WA058-M2A2T224	26.24	19.86	0.64	11.2646	30.1221	25.70324	8385
WA059-M2A2T224	26.21	19.89	0.59	11.4059	30.2132	22.75851	18456
WA060-M2A2T224	26.24	20	0.67	11.6449	30.5483	19.22175	42851
WA061-M2A2T224	26.7	20.5	0.62	12.0629	32.0948	17.0278	109535
WA062-M2A2T224	26.55	20.45	0.68	12.2529	31.9384	13.90013	1000000

Table A3.55: Fatigue Constants (a) and (b) of M_1, $[0,90°]_{3s}$

P_r	M_1, $[0,90°]_{3s}$		
	a (MPa)	b	Correlation factor
0	314.3	-0.1361	0.9926
0.25	242.5	-0.1359	0.9858
0.5	163.2	-0.133	0.9837
0.75	99.88	-0.1305	0.9811

Table A3.56: Fatigue Constants (a) and (b) of M_1, $[\pm 45°]_{3s}$

P_r	M_1, $[\pm 45°]_{3s}$		
	a (MPa)	**b**	**Correlation factor**
0	226.6	-0.1284	0.9953
0.25	169.7	-0.1264	0.9876
0.5	107.5	-0.1218	0.9845
0.75	62.09	-0.1181	0.9803

Table A3.57: Fatigue Constants (a) and (b) of M_2, $[0,90°]_{3s}$

P_r	M_2, $[0,90°]_{3s}$		
	a (MPa)	**b**	**Correlation factor**
0	484.4	-0.1612	0.9924
0.25	341.9	-0.1574	0.9911
0.5	229.2	-0.1548	0.9891
0.75	151.6	-0.1535	0.9878

Table A3.58: Fatigue Constants (a) and (b) of M_2, $[\pm 45°]_{3s}$

P_r	M_2, $[\pm 45°]_{3s}$		
	a (MPa)	**b**	**Correlation factor**
0	397.2	-0.1514	0.9843
0.25	263.3	-0.1501	0.9832
0.5	173.6	-0.1511	0.9837
0.75	102.7	-0.1512	0.9816

Table A3.59: Data of $[0,90°]_{2s}$ specimen tested under completely reversed pure bending R=-1 (Data adapted from Elmidany A. A. **[83]**)

Specimens code	σ_{max} [MPa]	Cycles to Failure (N)
9092071602	71.3	1804
9092071811	72	3237
9092072014	64.3	14106
9092081001	57.7	31013
9092081004	50.3	63411
9092081006	56	59413
9092081105	49	63522
9092092904	49.2	82416
9092100102	45.2	154216

Table A3.60: Data of $[\pm45°]_{2s}$ specimen tested under completely reversed pure bending R=-1 (Data adapted from Elmidany A. A. **[83]**)

Specimens code	σ_{max} [MPa]	Cycles to Failure (N)
4592102901	61	1510
4592102902	58	3714
4592102903	52.1	11260
4592102904	50	11528
4592102905	49	16206
4592102906	48	17523
4592102907	45	42980
4592102908	42.4	62227
4592102909	43.1	85669

Table A3.61: Data of $[0,90°]_{2s}$ specimen tested under completely reversed pure torsion R=-1 (Data adapted from Elmidany A. A. **[83]**)

Specimens code	σ_{max} [MPa]	Cycles to Failure (N)
9092072703	38.7	1328
9092072706	41.2	22.62
9092071913	40.8	2300
9092081002	37.9	7853
9092081003	37.8	10928
9092081104	32.6	11691
9092092801	36.4	17045
9092102601	33.1	62459
9092102602	30.5	87562

Table A3.62: Data of $[\pm 45°]_{2s}$ specimen tested under completely reversed pure torsion R=-1 (Data adapted from Elmidany A. A. [83])

Specimens code	σ_{max} [MPa]	Cycles to Failure (N)
4592112203	43.3	2221
4592112205	40	9208
4592112305	38.5	12305
4592112401	35.5	16088
4592112910	32.8	22160
4592120103	30.7	78616
4592120106	30	91318
4592120203	28.8	129592
4592120301	26.3	137978

Table A3.63: Data of $[0,90°]_{2s}$ specimen tested under completely reversed pure bending R=-1 (Data adapted from Nasr M. A. [84])

Specimens code	σ_{max} [MPa]	Cycles to Failure (N)
MN90-601-300901	82.052	757.5
MN90-613-300901	71.856	1882
MN90-610-041001	63.11	5380
MN90-605-041001	61.954	6752.5
MN90-608-031001	55.937	19300
MN90-609-031001	54.877	22467.5
MN90-612-081001	52.853	25240
MN90-606-101001	50.689	36820
MN90-607-101001	48.458	70125
MN90-611-131001	38.266	412080
MN90-604-171001	35.869	967956

Table A3.64: Data of $[0,90°]_{2s}$ specimen tested under completely reversed pure torsion R=-1 (Data adapted from Nasr M. A. [84])

Specimens code	σ_{max} [MPa]	Cycles to Failure (N)
MN90-107-290101	29.47	425
MN90-106-100201	29	612.5
MN90-113-290101	22.688	2322.5
MN90-112-080201	25.455	2781.25
MN90-114-010201	24.114	3325
MN90-115-080201	16.884	28946
MN90-108-080201	17.5	15322.5
MN90-110-010201	20.21	11550
MN90-103-090201	17.32	19000
MN90-111-100201	15.371	212797.5
MN90-109-030201	11.546	1023051

Table A3.65: Data of $[0,90°]_{2s}$ specimen tested under completely reversed pure bending (Data adapted from Elhadary M. M **[87]**)

Specimens code	σ_{max} [MPa]	Cycles to Failure (N)
MM90-1-01	35.45	1000000
MM90-1-02	43.06	409500
MM90-1-03	50.89	36093
MM90-1-04	53.89	28875
MM90-1-05	56.22	16152
MM90-1-06	62.24	6825
MM90-1-07	68.14	5915
MM90-1-08	70.70	3193
MM90-1-09	80.99	1181

Table A3.66: Data of $[0,90°]_{2s}$ specimen tested under completely reversed pure torsion (Data adapted from Elhadary M. M **[87]**)

Specimens code	σ_{max} [MPa]	Cycles to Failure (N)
MM90-1-10	11.56	1000000
MM90-1-11	14.64	220500
MM90-1-12	18.76	15837
MM90-1-13	19.75	13763
MM90-1-14	21.82	5118
MM90-1-15	22.97	2625
MM90-1-16	22.76	2301
MM90-1-17	23.40	2100
MM90-1-18	25.42	1575

Table A3.67: Data of $[\pm 45°]_{2s}$ specimen tested under completely reversed pure bending (Data adapted from Elhadary M. M **[87]**)

Specimens code	σ_{max} [MPa]	Cycles to Failure (N)
MM45-1-01	35.07	1000000
MM45-1-02	37.97	400150
MM45-1-03	41.69	85250
MM45-1-04	48.12	30450
MM45-1-05	54.27	18200
MM45-1-06	35.53	6825
MM45-1-07	55.62	4500
MM45-1-08	49.30	3000
MM45-1-09	62.28	1181

Table A3.68: Data of $[\pm 45°]_{2s}$ specimen tested under completely reversed pure torsion (Data adapted from Elhadary M. M **[87]**)

Specimens code	σ_{max} [MPa]	Cycles to Failure (N)
MM45-1-10	19.50	1000000
MM45-1-11	21.45	393750
MM45-1-12	24.30	241307
MM45-1-13	27.14	178815
MM45-1-14	30.28	50155
MM45-1-15	34.75	16555
MM45-1-16	37.41	3657
MM45-1-17	40.78	28875
MM45-1-18	43.79	2362

Table A3.69: Data of $[0,90°]_{2s}$ specimen tested under completely reversed pure bending (Data adapted from Mohamed S. Y **[88]**)

Specimens code	σ_{max} [MPa]	Cycles to Failure (N)
YS90001	75.13	1380
YS90002	71.92	4120
YS90003	65.86	6115
YS90004	63.43	9730
YS90005	59.06	18250
YS90006	56.83	29890
YS90007	52.47	45090
YS90008	40.24	519500
YS90009	36.3	1000000

Table A3.70: Data of $[0,90°]_{2s}$ specimen tested under completely reversed pure torsion (Data adapted from Mohamed S. Y **[88]**)

Specimens code	σ_{max} [MPa]	Cycles to Failure (N)
YS90010	27.26	820
YS90011	23.51	1950
YS90012	21.74	52.23
YS90013	17.98	12333
YS90014	17.58	18827
YS90015	16.83	26500
YS90016	15.94	67102
YS90017	12.42	549223
YS90018	10.58	1000000

Table A3.71: Data of $[\pm 45°]_{2s}$ specimen tested under completely reversed pure bending (Data adapted from Mohamed S. Y **[88]**)

Specimens code	σ_{max} [MPa]	Cycles to Failure (N)
YS45001	53.97	2225
YS45002	51.90	5147
YS45003	49.74	8630
YS45004	43.68	27190
YS45005	39.11	90138
YS45006	35.8	318220
YS45007	33.07	400130
YS45008	31.51	479445
YS45009	30.9	1000000

Table A3.72: Data of $[\pm 45°]_{2s}$ specimen tested under completely reversed pure torsion (Data adapted from Mohamed S. Y **[88]**)

Specimens code	σ_{max} [MPa]	Cycles to Failure (N)
YS45010	45.41	688
YS45011	40.78	2880
YS45012	38.88	3456
YS45013	35.61	13120
YS45014	30.38	49161
YS45015	27.54	182320
YS45016	25.12	238215
YS45017	22.03	372760
YS45018	19.2	1000000

Table A3.73: Data of $[30°,-60°]_{2s}$ specimen tested under completely reversed pure bending (Data adapted from Mohamed S. Y **[88]**)

Specimens code	σ_{max} [MPa]	Cycles to Failure (N)
YS30001	66.71	1945
YS30002	54.83	7123
YS30003	53.02	10456
YS30004	49.98	31470
YS30005	41.78	96690
YS30006	38.64	308111
YS30007	37.64	413665
YS30008	36.76	667332
YS30009	32.66	1000000

Table A3.74: Data of $[30°,-60°]_{2s}$ specimen tested under completely reversed pure torsion (Data adapted from Mohamed S. Y **[88]**)

Specimens code	σ_{max} [MPa]	Cycles to Failure (N)
YS30010	35.8	1500
YS30011	35.01	2625
YS30012	34.47	3000
YS30013	32.29	5250
YS30014	25.16	31500
YS30015	23.17	126000
YS30016	22.30	262500
YS30017	19.55	555418
YS30018	18.25	1000000

Table A3.75: Data of $[60°,-30°]_{2s}$ specimen tested under completely reversed pure bending (Data adapted from Mohamed S. Y **[88]**)

Specimens code	σ_{max} [MPa]	Cycles to Failure (N)
YS60001	66.34	2000
YS60002	51.38	27540
YS60003	48.19	42780
YS60004	46.14	65005
YS60005	45.36	78415
YS60006	39.63	302585
YS60007	41	425310
YS60008	36.42	730250
YS60009	34.8	1000000

Table A3.76: Data of $[60°,-30°]_{2s}$ specimen tested under completely reversed pure torsion (Data adapted from Mohamed S. Y **[88]**)

Specimens code	σ_{max} [MPa]	Cycles to Failure (N)
YS60010	37.1	2300
YS60011	36	3455
YS60012	34.06	4500
YS60013	30.1	6250
YS60014	28.04	31500
YS60015	24.23	135200
YS60016	22.49	285321
YS60017	22.36	576320
YS60018	19.84	1000000

Table A3.77: Data adapted from Amijima S. et al. **[72]**

(Obtained from Stress-Life Curve)

Pure bending		**Pure torsion**	
σ_{max} [MPa]	**Cycles to Failure (N)**	**σ_{max} [MPa]**	**Cycles to Failure (N)**
95.7	1000	44.33	1000
89.1	5000	42.9	5000
82.5	10000	41.47	10000
79.2	50000	38.61	50000
72.6	100000	35.75	100000
66	500000	32.89	500000
56.1	1000000	31.46	1000000

Table A3.78: Data adapted from Ahmed M.E. et al. **[75]**

(Obtained from Stress-Life Curve)

Pure bending		**Pure torsion**	
σ_{max} [MPa]	**Cycles to Failure (N)**	**σ_{max} [MPa]**	**Cycles to Failure (N)**
615	2000	55.21005	2000
540	10000	49.64621	10000
470	50000	47.42618	50000
435	100000	42.64677	100000
420	150000	40.73973	150000
400	300000	36.63415	300000
385	400000	34.99598	400000
380	500000	55.21005	500000
355	1000000	49.64621	1000000

Table A3.79: Data adapted from Atcholi KE. et al. **[151]**

(Obtained from Stress-Life Curve)

Pure bending		**Pure torsion**	
σ_{max} [MPa]	**Cycles to Failure (N)**	**σ_{max} [MPa]**	**Cycles to Failure (N)**
880	1000	220	1000
770	5000	192.5	5000
700	10000	175	10000
570	50000	142.5	50000
500	100000	125	100000

Table A3.80: Data adapted from Kawakami H. et al. **[152]**

(Obtained from Stress-Life Curve)

Pure bending		**Pure torsion**	
σ_{max} [MPa]	**Cycles to Failure (N)**	**σ_{max} [MPa]**	**Cycles to Failure (N)**
169.1646	1000	55.21005	1000
136.4135	5000	49.64621	5000
124.3396	10000	47.42618	10000
100.2668	50000	42.64677	50000
91.3923	100000	40.73973	100000
73.69827	500000	36.63415	500000
67.1753	1000000	34.99598	1000000

Table A3.81: Data adapted from Önder A. **[8]** (static pressure test)

winding Angle	**Inner Diameter (mm)**	**Thickness (mm)**	**Total length (mm)**	**Maximum Pressure Recorded $P_{i_{max}}$ (bars)**
$[\pm 45°]_2$	***50***	***0.16***	***400***	***56.6***
$[\pm 55°]_2$				***102.4***
$[\pm 60°]_2$				***74***
$[\pm 75°]_2$				***32.2***
$[90°]_2$				***17.4***

Table A3.82: Data adapted from Tolga L. **[52]** (static pressure test)

winding Angle	**Inner Diameter (mm)**	**Thickness (mm)**	**Maximum Pressure Recorded $P_{i_{max}}$ (bars)**
$[\pm 30°]_2$	***75***	***3***	***88***
$[\pm 45°]_2$			***140***
$[\pm 55°]_2$			***182***
$[\pm 60°]_2$			***176***
$[\pm 75°]_2$			***134***
$[\pm 90°]_2$			***122***

Table A3.83: Data adapted from Tolga L. **[52]** (static pressure test)

winding Angle	**Inner Diameter (mm)**	**Thickness (mm)**	**Maximum Pressure Recorded $P_{i_{max}}$ (bars)**
$[+55°/-55°]_2$	***75***	***3***	***142.4***
$[+55°/-55°]_S$			***234.6***
$[+88°/-11°/+11°/-88°]_2$			***237.4***
$[+66°/-40°/+40°/-66°]_2$			***117.3***

Table A3.84: Data adapted from Erkal S. **[148]** (static pressure test)

winding Angle	**Inner Diameter (mm)**	**Thickness (mm)**	**Total length (mm)**	**Maximum Pressure Recorded $P_{i_{max}}$ (bars)**
[±45°]₂	***50***	***0.16***	***400***	***108***
[±55°]₂				***102.4***
[±60°]₂				***74***
[±75°]₂				***33.2***
[±90°]₂				***17.4***

Table A3.85: Failure criteria / Theories of failure **[83]**

No.	**Name**	**Mathematical formula**
1	Max. stress	$\sigma_1 = F_1\ ,\quad \sigma_2 = F_2,\quad \sigma_6 = F_6$
2	Max. strain	$\sigma_1 = F_1 + \upsilon_{12}\sigma_2\ ,\ \ \sigma_2 = F_2 + \upsilon_{12}\frac{E_2}{E_1}\sigma_1,\quad \sigma_6 = F_6$
3	Hill criterion	$\left(\frac{\sigma_1}{F_1}\right)^2 - \left(\frac{1}{{F_1}^2} + \frac{1}{{F_2}^2}\right)\sigma_1\sigma_2 + \left(\frac{\sigma_2}{F_2}\right)^2 + \left(\frac{\sigma_6}{F_6}\right)^2 = 1$
4	Tsai-Hill	$\left(\frac{\sigma_1}{F_1}\right)^2 - \left(\frac{\sigma_1\sigma_2}{{F_1}^2}\right) + \left(\frac{\sigma_2}{F_2}\right)^2 + \left(\frac{\sigma_6}{F_6}\right)^2 = 1$
5	Norris interaction	$\left(\frac{\sigma_1}{F_1}\right)^2 + \left(\frac{\sigma_2}{F_2}\right)^2 + \left(\frac{\sigma_6}{F_6}\right)^2 = 1$
6	Norris distortional energy	$\left(\frac{\sigma_1}{F_1}\right)^2 - \left(\frac{\sigma_1\sigma_2}{F_1F_2}\right) + \left(\frac{\sigma_2}{F_2}\right)^2 + \left(\frac{\sigma_6}{F_6}\right)^2 = 1$ or $\left(\frac{\sigma_1}{F_1}\right)^2 = 1$ or $\left(\frac{\sigma_2}{F_2}\right)^2 = 1$
7	Hoffman	$\left(\frac{{\sigma_1}^2 - \sigma_1\sigma_2}{F_{1t}F_{1c}}\right) + \left(\frac{{\sigma_2}^2}{F_{2t}F_{2c}}\right) + \left(\frac{F_{1c} - F_{1t}}{F_{1t}F_{1c}}\right)\sigma_1 + \left(\frac{F_{2c} - F_{2t}}{F_{2t}F_{2c}}\right)\sigma_2 + \left(\frac{\sigma_6}{F_6}\right)^2 = 1$
8	Modified Marin	$\left(\frac{{\sigma_1}^2 - K_2\sigma_1\sigma_2}{F_{1t}F_{1c}}\right) + \left(\frac{{\sigma_2}^2}{F_{2t}F_{2c}}\right) + \left(\frac{F_{1c} - F_{1t}}{F_{1t}F_{1c}}\right)\sigma_1 + \left(\frac{F_{2c} - F_{2t}}{F_{2t}F_{2c}}\right)\sigma_2 + \left(\frac{\sigma_6}{F_6}\right)^2 = 1$ Where: K_2 is floating constant.

9	Tsai-Wu	$\left(\frac{1}{F_{1t}}-\frac{1}{F_{1c}}\right)\sigma_1+\left(\frac{1}{F_{2t}}-\frac{1}{F_{2c}}\right)\sigma_2+\left(\frac{{\sigma_1}^2}{F_{1t}F_{1c}}\right)+\left(\frac{{\sigma_2}^2}{F_{2t}F_{2c}}\right)$ $+(2H_{12}\sigma_1\sigma_2)+\left(\frac{\sigma_6}{F_6}\right)^2=1$ And the following condition must be fulfilled, for stability: $\frac{1}{F_{1t}F_{1c}F_{2t}F_{2c}}-{H_{12}}^2\geq 0$
10	Ashkenazi	$\left(\frac{\sigma_1}{F_1}\right)^2+\left(\frac{\sigma_2}{F_2}\right)^2+\left(\frac{\sigma_6}{F_6}\right)^2+(2F_{12}\sigma_1\sigma_2)=1$ $F_{12}=0.5\left(\frac{4}{{\sigma_X}^2}-\frac{1}{{F_1}^2}-\frac{1}{{F_2}^2}-\frac{1}{{F_6}^2}\right)$ Where: σ_X is the global stress of 45° in tension.
11	Tsai-Hahn	The same formula as Tsai-Wu but H_{12} takes the form: $H_{12}=-0.5\sqrt{\frac{1}{F_{1t}F_{1c}F_{2t}F_{2c}}}$
12	Cowin	The same formula as Tsai-Wu but H_{12} takes the form: $H_{12}=\sqrt{\frac{1}{F_{1t}F_{1c}F_{2t}F_{2c}}}-\frac{1}{2{F_6}^2}$
13	Fischer	$\left(\frac{\sigma_1}{F_1}\right)^2-C\left(\frac{\sigma_1\sigma_2}{{F_1}^2}\right)+\left(\frac{\sigma_2}{F_2}\right)^2+\left(\frac{\sigma_6}{F_6}\right)^2=1$ Where: $k=\frac{E_1(1+\upsilon_{21})+E_2(1+\upsilon_{12})}{2\sqrt{E_1E_2(1+\upsilon_{21})(1+\upsilon_{12})}}$
14	El-Midany **[83]**	$\left(\frac{\sigma_1}{F_1}\right)^2+\left(\frac{\sigma_2}{F_2}\right)^2+\left(\frac{\sigma_6}{F_6}\right)^2+2(\sigma_1\sigma_2)\left(\frac{2}{A_{45}^2}-\frac{1}{F_1^2}-\frac{1}{2F_6^2}\right)=1$ Where: A_{45} is the strength of the *[±45°]* specimens under pure bending test
		$\left(\frac{\tau_{eq}}{F_{6s}}\right)^2=1$ (for $[0^o,90^o]_{2s}$) $3\left(\frac{\tau_{eq}}{F_{1s}}\right)^2+\left(\frac{SWT^2}{F_{1s}F_{1f}}\right)=1$

15	Nasr **[84]**	(for $[\pm 45^{o}]_{2s}$) Where: $(\tau_{eq})_{[0°,90°]} = \tau_m + K_{mn}\left(\frac{\tau_a}{S_{fs}}\right)S_{us}$, $(\tau_{eq})_{[\pm 45°]} = \tau_m + \left(\frac{\tau_a}{S_{fs}}\right)S_{us}$, $K_{mn} = \frac{S_{us} - C_{mn}\,S_{fs}}{S_{us}}$, $C_{mn} = \frac{1+R}{1-R}$, R is the stress ratio between minimum and maximum stress, F_{1s} is the local static strength in the fiber direction, F_{6s} is the local static shear strength, F_{1f} is the local fatigue strength in the fiber direction, S_{fs} is the torsional fatigue shear strength, S_{us} is the ultimate global shear strength, τ_m, τ_a are the mean and amplitude global shear stress, respectively, τ_{eq} is equivalent global static shear stress, SWT represents the Smith-Watson-Topper parameter (SWT $= \sqrt{\tau_{max}\,\tau_a}$)
16	El-Hadary **[86]**	$\left(\frac{\sigma_1}{F_1}\right)^2 + \left(\frac{\sigma_2}{F_2}\right)^2 + \left(\frac{\sigma_6}{F_6}\right)^2 + K_1\left(\frac{\sigma_1\sigma_2}{F_1F_2}\right) + K_2\left(\frac{\sigma_1\sigma_6}{F_1F_6}\right) + K_3\left(\frac{\sigma_2\sigma_6}{F_2F_6}\right) = 1$ Where: $K_1 = -0.003\left(\frac{A}{B}\right) + 12.5(R) + 10$, $K_2 = -1.97\left(\frac{A}{B}\right)^2 + 5.27\left(\frac{A}{B}\right) - 0.37(R) - 2.6$, $K_3 = -0.33\left(\frac{A}{B}\right) - 11.4(R) - 8$, R is the stress ratio between minimum and maximum stress,

		$\left(\frac{A}{B}\right)$ is the ratio between amplitude global bending and torsional stress.
17	El-Hadary **[87]**	$\left(\frac{\sigma_1}{F_1}\right)^2+\left(\frac{\sigma_2}{F_2}\right)^2+\left(\frac{\sigma_6}{F_6}\right)^2-\left(\frac{\sigma_1\sigma_2}{F_1F_2}\right)+H_{16}\left(\frac{\sigma_1\sigma_6}{F_1F_6}\right)=1$ Where: $H_{16}=\frac{Z+R}{Z+q}$, $q=\left(\frac{A}{B}\right)$, R is the stress ratio between minimum and maximum stress, Z is the phase shift between bending moment and torque, $\left(\frac{A}{B}\right)$ is the ratio between amplitude global bending and torsional stress.
18	Mohamed **[88]**	$\left(\frac{\sigma_1}{F_1}\right)^2+\left(\frac{\sigma_2}{F_2}\right)^2+\left(\frac{\sigma_6}{F_6}\right)^2-K_1\left(\frac{\sigma_1\sigma_2}{F_1F_2}\right)+K_2\left(\frac{\sigma_1\sigma_6}{F_1F_6}\right)=1$ (for negative stress) $\left(\frac{\sigma_1}{F_1}\right)^2+\left(\frac{\sigma_2}{F_2}\right)^2+\left(\frac{\sigma_6}{F_6}\right)^2-\left(\frac{\sigma_1\sigma_2}{F_1F_2}\right)+K_3\left(\frac{\sigma_1\sigma_6}{F_1F_6}\right)=1$ (for positive stress) Where: $K_1=\theta\left(\frac{S_{us}}{S_{es\ (pure\ \ torsion\ )}}\right)$, $K_2=\left(\frac{(\theta-R)}{\left(\theta-\left(\frac{A}{B}\right)\right)}\right)\left(\frac{S_{us}}{S_u}\right)_{[0,90°]}$, $K_3=R\left(\theta^2+\frac{1}{\left(\frac{A}{B}\right)}\right)\left(\frac{S_u^2}{A_\theta\ S_{es\ (pure\ \ torsion\ )}}\right)$, R is the stress ratio between minimum and maximum stress, S_{us} is the ultimate global shear strength, S_u is the ultimate global normal strength, $\left(\frac{A}{B}\right)$ is the ratio between amplitude global bending and

		torsional stress, θ is the fiber orientation angle, S_{es} is the endurance shear strength A_θ is the strength of the specimens corresponding on fiber orientation.

Where:

σ_1 and σ_2 are the local stress components in directions (1) and (2), respectively.

σ_6 is the local shear component.

F_{1t} & F_{1c} and F_{2t} & F_{2c} are the local tension and compression strength components in directions (1) and (2), respectively.

F_6 is the local shear strength component.

υ_{12} and υ_{21} represent Poisson's ratios in the local directions.

E_1 and E_2 are the local modullii of elasticity in directions (1) and (2), respectively.

APPENDIX (4)

STRESSES IN THICK WALLED AND MULTILAYER TUBES

A4.1 Theory of thick-walled cylinders

Figure A4.1 show stressed Thick-walled cylinder with radius *r*, the solid line is unstrained cylinder and the dash line is strained cylinder.

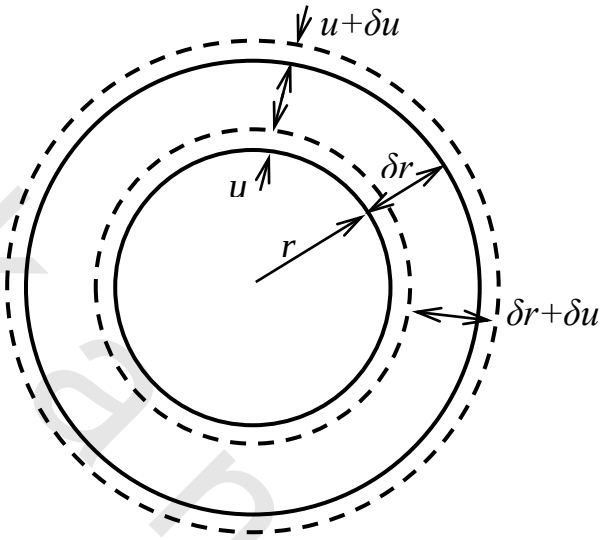

Figure A4.1.Thick-walled cylinder, the solid line is unstrained cylinder and the dash line is strained cylinder.

$$\because \varepsilon_H = \frac{2\pi(r+u) - 2\pi r}{2\pi r} = \frac{u}{r},$$

$$\because \varepsilon_L = constant,$$

$$\because \varepsilon_r = \frac{(\delta r + \delta u) - \delta r}{\delta r} = \frac{\delta u}{\delta r}$$

Where:

ε_H: Hoop strain (diameteral strain),

ε_L: Longitudinal strain,

ε_r: Redial strain.

By apply stress-strain relation (tri-axial tresses):

$$E\varepsilon_L = \sigma_L - \upsilon(\sigma_H + \sigma_r) = \sigma_L - \upsilon(\sigma_H - P) \quad \text{(A4.1)}$$

$$E\varepsilon_H = E\frac{u}{r} = \sigma_H - \upsilon(\sigma_L + \sigma_r) = \sigma_H - \upsilon(\sigma_L - P) \quad \text{(A4.2)}$$

$$E\varepsilon_r = E\frac{du}{dr} = \sigma_r - \upsilon(\sigma_H + \sigma_L) = -P - \upsilon(\sigma_H + \sigma_L) \quad \text{(A4.3)}$$

By derivative equation A4.2 w.r.t *r*:

$\because Eu = r[\sigma_H - \upsilon\sigma_L + \upsilon P]$

$\therefore E\frac{du}{dr} = [\sigma_H - \upsilon\sigma_L + \upsilon P] + r\frac{d\sigma_H}{dr} - \upsilon r\frac{d\sigma_L}{dr} + \upsilon r\frac{dP}{dr}$ (A4.4)

Substitute equation A4.4 into A4.3:

$$\therefore -P - \upsilon\sigma_H - \upsilon\sigma_L = \sigma_H - \upsilon\sigma_L + \upsilon P + r\frac{d\sigma_H}{dr} - \upsilon r\frac{d\sigma_L}{dr} + \upsilon r\frac{dP}{dr}$$

$\therefore (\sigma_H + P)(1+\upsilon) + r\frac{d\sigma_H}{dr} - \upsilon r\frac{d\sigma_L}{dr} + \upsilon r\frac{dP}{dr} = 0$ (A4.5)

By derivative equation A4.1 w.r.t *r*:

$\because \varepsilon_L = constant$

$$\therefore \frac{d\varepsilon_L}{dr} = 0 = \frac{d\sigma_L}{dr} - \upsilon\frac{d\sigma_H}{dr} + \upsilon\frac{dP}{dr}$$

$\therefore \frac{d\sigma_L}{dr} = \upsilon\frac{d\sigma_H}{dr} - \upsilon\frac{dP}{dr}$ (A4.6)

Substitute equation A4.6 into A4.5:

$\therefore (\sigma_H + P)(1+\upsilon) + r\frac{d\sigma_H}{dr} - \upsilon^2 r\frac{d\sigma_H}{dr} + \upsilon^2 r\frac{dP}{dr} + \upsilon r\frac{dP}{dr} = 0$

$\therefore (\sigma_H + P)(1+\upsilon) + r\frac{d\sigma_H}{dr}(1-\upsilon^2) + \upsilon r\frac{dP}{dr}(1+\upsilon) = 0$

$\therefore (\sigma_H + P) + r\frac{d\sigma_H}{dr}(1-\upsilon) + \upsilon r\frac{dP}{dr} = 0$ (A4.7)

By equilibrium of cylinder element shown in the Figure A4.2:

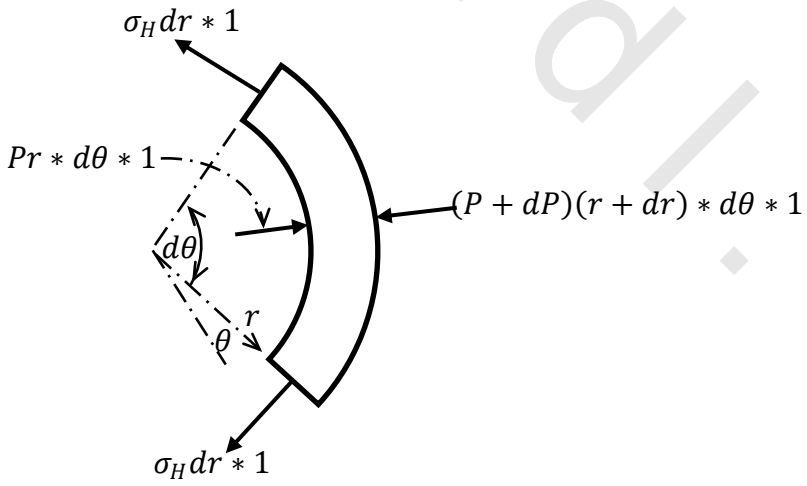

Figure A4.2 Thick-walled cylinder element.

$\therefore (P + dP)(r + dr) * d\theta - Pr * d\theta + 2\sigma_H dr \sin\frac{d\theta}{2} = 0$

Neglect the term of $\left(\sin\frac{d\theta}{2}\right)$ is very small:

$\therefore Pr + Pdr + rdP + dPdr - Pr + \sigma_H dr = 0$

Neglect the term of $(dPdr)$ is very small:

$$\therefore Pdr + rdP + \sigma_H dr = 0$$

$$\therefore (\sigma_H + P) + r\frac{dP}{dr} = 0 \quad \text{(A4.8)}$$

Substitute equation A4.8 into A4.7:

$$\therefore r(1-\upsilon)\frac{d\sigma_H}{dr} - r(1-\upsilon)\frac{dP}{dr} = 0 \quad \text{(A4.9)}$$

By solve the differential equation A4.9:

$$\therefore \sigma_H - P = constant$$

Where *C* is the constant we can be assumed equal $2K_1$:

$$\therefore \sigma_H - P = 2K_1 \quad \text{(A4.10)}$$

Substitute equation A4.8 into A4.10:

$$\therefore 2P + r\frac{dP}{dr} = -2K_1$$

$$\therefore \frac{1}{r}\frac{dPr^2}{dr} = -2K_1$$

$$\therefore \int dPr^2 = \int -2K_1\, rdr$$

$$\therefore Pr^2 = -2K_1\left(\frac{r^2}{2}\right) + K_2$$

$$\therefore P = -K_1 + \frac{K_2}{r^2}$$

$$\therefore \sigma_r = -P = K_1 - \frac{K_2}{r^2} \quad \text{(A4.11)}$$

From equation (A4.10):

$$\therefore \sigma_H = K_1 + \frac{K_2}{r^2} \quad \text{(A4.12)}$$

Finally,

$$\sigma_r = K_1 - \frac{K_2}{r^2} = -P,$$

$$\sigma_H = K_1 + \frac{K_2}{r^2}$$

$$\sigma_L = constant$$

Where:

σ_H: Hoop stress,

σ_L: Longitudinal stress,

σ_r: Redial stress,

K_1, K_2: Constants required from the cylinder boundary conditions.

By apply the general boundary conditions in stresses equation:

1. At $r = r_i$ $\quad \therefore \sigma_r = -P_i$
2. At $r = r_o$ $\quad \therefore \sigma_r = -P_o$

$$\therefore -P_i = K_1 - \frac{K_2}{{r_i}^2} \tag{A4.13}$$

$$\therefore -P_o = K_1 - \frac{K_2}{{r_o}^2} \tag{A4.14}$$

From equations A4.13 and A4.14:

$$\therefore A = -P_i + \frac{K_2}{{r_i}^2}$$

$$\therefore K_2 \left(\frac{1}{{r_i}^2} - \frac{1}{{r_o}^2}\right) = P_i - P_o$$

$$\therefore K_2 \left(\frac{{r_i}^2 - {r_o}^2}{{r_i}^2 {r_o}^2}\right) = P_i - P_o$$

$$\therefore K_2 = \frac{(P_i - P_o){r_i}^2 {r_o}^2}{{r_i}^2 - {r_o}^2}$$

$$\therefore K_1 = -P_i + \frac{(P_i - P_o){r_o}^2}{{r_i}^2 - {r_o}^2}$$

$$\therefore K_1 = \frac{P_i({r_i}^2 - {r_o}^2) + (P_i - P_o){r_o}^2}{{r_o}^2 - {r_i}^2}$$

Substitute the constants K_1, K_2 into stresses equations:

$$\therefore \sigma_H = \frac{P_i({r_i}^2 - {r_o}^2) + (P_i - P_o){r_o}^2}{{r_o}^2 - {r_i}^2} - \frac{(P_i - P_o){r_i}^2 {r_o}^2}{r^2({r_o}^2 - {r_i}^2)}$$

$$\therefore \sigma_H = \frac{P_i({r_i}^2 - {r_o}^2) + (P_i - P_o){r_o}^2 + (P_o - P_i)\left(\frac{{r_i}^2 {r_o}^2}{r^2}\right)}{{r_o}^2 - {r_i}^2}$$

$$\therefore \sigma_H = \frac{P_i {r_i}^2 - P_o {r_o}^2 - (P_o - P_i)\left(\frac{{r_i}^2 {r_o}^2}{r^2}\right)}{{r_o}^2 - {r_i}^2}, \tag{A4.15}$$

$$\therefore \sigma_r = \frac{P_i {r_i}^2 - P_o {r_o}^2 + (P_o - P_i)\left(\frac{{r_i}^2 {r_o}^2}{r^2}\right)}{{r_o}^2 - {r_i}^2}, \tag{A4.16}$$

$$\because \tau_{max} = \frac{\sigma_H - \sigma_r}{2} \qquad at\ r = r_o$$

$$\therefore \tau_{max} = \frac{(P_i - P_o){r_i}^2 {r_o}^2}{{r_o}^2({r_o}^2 - {r_i}^2)} \tag{A4.17}$$

$$\therefore \sigma_L = \frac{P_i {r_i}^2 - P_o {r_o}^2}{{r_o}^2 - {r_i}^2} \quad for\ closed\ cylinder \tag{A4.18}$$

$\therefore \sigma_L = 0 \quad for\ open\ cylinder$

From equation A4.2:

$$\therefore E\frac{u}{r} = [\sigma_H - \upsilon(\sigma_L - P)]$$

$$\therefore \delta = u = \frac{1}{E} r[\sigma_H - \upsilon(\sigma_L - P)]$$

$$\therefore \delta = \frac{1}{E} r\left[\frac{P_i {r_i}^2 - P_o {r_o}^2}{{r_o}^2 - {r_i}^2} - \frac{(P_o - P_i)\left(\frac{{r_i}^2 {r_o}^2}{r^2}\right)}{{r_o}^2 - {r_i}^2} - \upsilon\frac{P_i {r_i}^2 - P_o {r_o}^2}{{r_o}^2 - {r_i}^2} - \upsilon\frac{(P_o - P_i)\left(\frac{{r_i}^2 {r_o}^2}{r^2}\right)}{{r_o}^2 - {r_i}^2}\right]$$

$$\therefore \delta = \frac{1}{E} r\left[\frac{P_i {r_i}^2 - P_o {r_o}^2}{{r_o}^2 - {r_i}^2}(1-\upsilon) - \frac{(P_o - P_i){r_i}^2 {r_o}^2}{r^2({r_o}^2 - {r_i}^2)}(1+\upsilon)\right]$$

$$\therefore \delta = \frac{(1-\upsilon)}{E}\left(\frac{P_i {r_i}^2 - P_o {r_o}^2}{{r_o}^2 - {r_i}^2}\right) r + \frac{(1+\upsilon)}{E}\left(\frac{(P_i - P_o){r_i}^2 {r_o}^2}{r({r_o}^2 - {r_i}^2)}\right) \quad \text{(A4.19)}$$

Special case (tube):

For the tube $P_o = 0$

$$\therefore \sigma_H = \frac{P_i {r_i}^2}{{r_o}^2 - {r_i}^2}\left(1 + \frac{{r_o}^2}{r^2}\right), \quad \text{(A4.20)}$$

$$\therefore \sigma_r = \frac{P_i {r_i}^2}{{r_o}^2 - {r_i}^2}\left(1 - \frac{{r_o}^2}{r^2}\right), \quad \text{(A4.21)}$$

$$\therefore \sigma_L = \frac{P_i {r_i}^2}{{r_o}^2 - {r_i}^2} \quad for\ closed\ cylinder \quad \text{(A4.22)}$$

$\therefore \sigma_L = 0 \quad for\ open\ cylinder$

$$\therefore \delta = \frac{(1-\upsilon)}{E}\left(\frac{P_i {r_i}^2}{{r_o}^2 - {r_i}^2}\right) r + \frac{(1+\upsilon)}{E}\left(\frac{P_i {r_i}^2 {r_o}^2}{r({r_o}^2 - {r_i}^2)}\right) \quad \text{(A4.23)}$$

A4.2 Theory of multilayer thick-walled pipes

The outside radius *b* of the internal layer was larger than the inside radius of the middle layer by an amount $\delta_{1\text{-}2}$, creating the interface pressure $P_{1\text{-}2}$ between the internal layer and the middle layer after assembly. Also the outside radius *b* of the middle layer was larger than the inside radius of the external layer by an amount $\delta_{2\text{-}3}$, creating the interface pressure $P_{2\text{-}3}$ between the middle layer and the external layer after assembly, see Figure A4.3. Its value may be obtained from:

$\delta_{1\text{-}2}$ = Increase in inner radius of middle layer (δ_1) + Decrease in outer radius of internal layer (δ_2) (A4.24)

$\delta_{2\text{-}3}$ = Increase in inner radius of external layer (δ_3) + Decrease in outer radius of middle layer (δ_4) (A4.25)

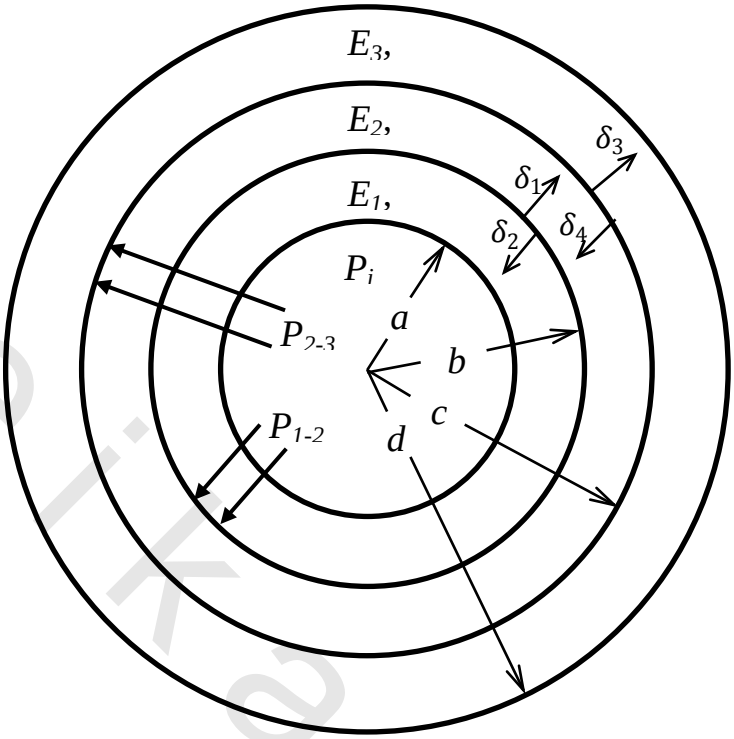

Figure A4.3 Three-layer thick-walled pipes.

Calculation of interface pressures and hoop stresses

1) For middle layer $\delta_{1\text{-}2}$:

In equation A4.19 putting:

$P_o = P_{2-3}$, $P_i = P_{1-2}$,

$r = r_i = b$, $r_o = c$.

$$\therefore \delta_1 = \frac{(1-\upsilon_2)}{E_2}\left(\frac{P_{1-2}b^2 - P_{2-3}c^2}{c^2-b^2}\right)b + \frac{(1+\upsilon_2)}{E_2}\left(\frac{(P_{1-2}-P_{2-3})b^2c^2}{b(c^2-b^2)}\right) \quad \text{(A4.26)}$$

2) For internal layer :

In equation A4.19 putting:

$P_o = P_{1-2}$, $P_i = P$,

$r = r_o = b$, $r_i = a$.

$$\therefore \delta_2 = -\left[\frac{(1-\upsilon_1)}{E_1}\left(\frac{Pa^2 - P_{1-2}b^2}{b^2-a^2}\right)b + \frac{(1+\upsilon_1)}{E_1}\left(\frac{(P-P_{1-2})a^2b^2}{b(b^2-a^2)}\right)\right] \quad \text{(A4.27)}$$

3) For external layer:

In equation A4.19 putting:

$P_o = 0$, $P_i = P_{2-3}$,

$$r = r_i = c, \qquad r_o = d.$$

$$\therefore \delta_3 = \frac{(1-v_3)}{E_3}\left(\frac{P_{2-3}c^2}{d^2-c^2}\right)c + \frac{(1+v_3)}{E_3}\left(\frac{P_{2-3}c^2d^2}{c(d^2-c^2)}\right) \quad \text{(A4.28)}$$

4) For middle layer $\delta_{2\text{-}3}$:

In equation A4.19 putting:

$$P_o = P_{2-3}, \qquad P_i = P_{1-2},$$

$$r = r_o = c, \qquad r_i = b.$$

$$\therefore \delta_4 = -\left[\frac{(1-v_2)}{E_2}\left(\frac{P_{1-2}b^2-P_{2-3}c^2}{c^2-b^2}\right)c + \frac{(1+v_2)}{E_2}\left(\frac{(P_{1-2}-P_{2-3})b^2c^2}{c(c^2-b^2)}\right)\right] \quad \text{(A4.29)}$$

Substitute the values of δ_1 and δ_2 into equation A4.24:

$$\therefore \delta_{1-2} = \frac{(1-v_2)}{E_2}\left(\frac{P_{1-2}b^2-P_{2-3}c^2}{c^2-b^2}\right)b + \frac{(1+v_2)}{E_2}\left(\frac{(P_{1-2}-P_{2-3})b^2c^2}{b(c^2-b^2)}\right) - \frac{(1-v_1)}{E_1}\left(\frac{Pa^2-P_{1-2}b^2}{b^2-a^2}\right)b - \frac{(1+v_1)}{E_1}\left(\frac{(P-P_{1-2})a^2b^2}{b(b^2-a^2)}\right)$$

$$\therefore \delta_{1-2} = \frac{1}{E_2(c^2-b^2)}\left[(1-v_2)(P_{1-2}b^2 - P_{2-3}c^2)b + \left((1+v_2)(P_{1-2}-P_{2-3})bc^2\right)\right] - \frac{1}{E_1(b^2-a^2)}\left[(1-v_1)(Pa^2 - P_{1-2}b^2)b + \left((1+v_1)(P-P_{1-2})a^2b\right)\right]$$

$$\therefore \delta_{1-2} = \frac{b}{E_2(c^2-b^2)}[P_{1-2}b^2(1-v_2) - P_{2-3}c^2(1-v_2) + P_{1-2}c^2(1+v_2) - P_{2-3}c^2(1+v_2)] - \frac{b}{E_1(b^2-a^2)}[Pa^2(1-v_1) - P_{1-2}b^2(1-v_1) + Pa^2(1+v_1) - P_{1-2}a^2(1+v_1)]$$

$$\therefore \delta_{1-2} = \frac{P_{1-2}b}{E_2(c^2-b^2)}[b^2(1-v_2) + c^2(1+v_2)] - \frac{P_{2-3}b}{E_2(c^2-b^2)}[c^2(1-v_2) + c^2(1+v_2)] - \frac{Pb}{E_1(b^2-a^2)}[a^2(1-v_1) + a^2(1+v_1)] + \frac{P_{1-2}b}{E_1(b^2-a^2)}[b^2(1-v_1) + a^2(1+v_1)]$$

$$\therefore \delta_{1-2} = P_{1-2}b\left(\frac{1}{E_2(c^2-b^2)}[b^2(1-v_2) + c^2(1+v_2)] + \frac{1}{E_1(b^2-a^2)}[b^2(1-v_1) + a^2(1+v_1)]\right) - P_{2-3}b\left(\frac{1}{E_2(c^2-b^2)}[c^2(1-v_2) + c^2(1+v_2)]\right) - Pb\left(\frac{1}{E_1(b^2-a^2)}[a^2(1-v_1) + a^2(1+v_1)]\right)$$

$$\therefore \delta_{1-2} = P_{1-2}b\left(\frac{1}{E_2(c^2-b^2)}[b^2(1-\upsilon_2)+c^2(1+\upsilon_2)]+\frac{1}{E_1(b^2-a^2)}[b^2(1-\upsilon_1)+ a^2(1+\upsilon_1)]\right)-P_{2-3}b\left(\frac{2c^2}{E_2(c^2-b^2)}\right)-Pb\left(\frac{2a^2}{E_1(b^2-a^2)}\right) \quad \text{(A4.30)}$$

Substitute the values of $\delta_3$and δ_4 into equation A4.25:

$$\therefore \delta_{2-3} = \frac{(1-\upsilon_3)}{E_3}\left(\frac{P_{2-3}c^2}{d^2-c^2}\right)c+\frac{(1+\upsilon_3)}{E_3}\left(\frac{P_{2-3}c^2d^2}{c(d^2-c^2)}\right)-\frac{(1-\upsilon_2)}{E_2}\left(\frac{P_{1-2}b^2-P_{2-3}c^2}{c^2-b^2}\right)c-\frac{(1+\upsilon_2)}{E_2}\left(\frac{(P_{1-2}-P_{2-3})b^2c^2}{c(c^2-b^2)}\right)$$

$$\therefore \delta_{2-3} = \frac{c}{E_3(d^2-c^2)}\left[\left((1-\upsilon_3)P_{2-3}c^2\right)+\left((1+\upsilon_3)P_{2-3}d^2\right)\right]-\frac{c}{E_2(c^2-b^2)}\left[\left((1-\upsilon_2)P_{1-2}b^2-P_{2-3}c^2\right)+\left((1+\upsilon_2)(P_{1-2}-P_{2-3})b^2\right)\right]$$

$$\therefore \delta_{2-3} = \frac{c}{E_3(d^2-c^2)}[P_{2-3}c^2-\upsilon_3P_{2-3}c^2+P_{2-3}d^2+\upsilon_3P_{2-3}d^2]-\frac{c}{E_2(c^2-b^2)}[2P_{1-2}b^2-P_{2-3}c^2+\upsilon_2P_{2-3}c^2-P_{2-3}b^2-\upsilon_2P_{2-3}b^2]$$

$$\therefore \delta_{2-3} = \frac{P_{2-3}c}{E_3(d^2-c^2)}[c^2-\upsilon_3c^2+d^2+\upsilon_3d^2]-\frac{P_{2-3}c}{E_2(c^2-b^2)}[\upsilon_2c^2-c^2-b^2-\upsilon_2b^2]-\frac{2P_{1-2}b^2c}{E_2(c^2-b^2)}$$

$$\therefore \delta_{2-3} = P_{2-3}c\left[\frac{1}{E_3(d^2-c^2)}[c^2-\upsilon_3c^2+d^2+\upsilon_3d^2]-\frac{1}{E_2(c^2-b^2)}[\upsilon_2c^2-c^2-b^2-\upsilon_2b^2]\right]-\frac{2P_{1-2}b^2c}{E_2(c^2-b^2)} \quad \text{(A4.31)}$$

From equation A4.31:

$$\therefore P_{2-3} = \frac{\delta_{2-3}+\frac{2P_{1-2}b^2c}{E_2(c^2-b^2)}}{c\left[\frac{[c^2-\upsilon_3c^2+d^2+\upsilon_3d^2]}{E_3(d^2-c^2)}-\frac{[\upsilon_2c^2-c^2-b^2-\upsilon_2b^2]}{E_2(c^2-b^2)}\right]}, \quad \delta_{2-3} \text{ is very small.}$$

$$\therefore P_{2-3} = \frac{\frac{2P_{1-2}b^2}{E_2(c^2-b^2)}}{\frac{1}{E_3}\left[\frac{[c^2-\upsilon_3c^2+d^2+\upsilon_3d^2]}{(d^2-c^2)}\right]-\frac{1}{E_2}\left[\frac{[\upsilon_2c^2-c^2-b^2-\upsilon_2b^2]}{(c^2-b^2)}\right]}$$

$$\therefore P_{2-3} = \frac{\frac{2P_{1-2}b^2}{E_2(c^2-b^2)}}{\frac{1}{E_3}\left[\frac{[(d^2+c^2)+\upsilon_3(d^2-c^2)]}{(d^2-c^2)}\right]-\frac{1}{E_2}\left[\frac{[\upsilon_2(c^2-b^2)-(c^2+b^2)]}{(c^2-b^2)}\right]}$$

$$\therefore P_{2-3} = \frac{2P_{1-2}b^2}{E_2(c^2-b^2)\left(\frac{1}{E_3}\left[\frac{(d^2+c^2)}{(d^2-c^2)}+\upsilon_3\right]+\frac{1}{E_2}\left[\frac{(c^2+b^2)}{(c^2-b^2)}-\upsilon_2\right]\right)}$$

$$\therefore P_{2-3} = \frac{2P_{1-2}}{E_2\left(\frac{c^2}{b^2}-1\right)\left(\frac{1}{E_3}\left[\frac{\left(\frac{d^2}{c^2}+1\right)}{\left(\frac{d^2}{c^2}-1\right)}+\upsilon_3\right]+\frac{1}{E_2}\left[\frac{\left(\frac{c^2}{b^2}+1\right)}{\left(\frac{c^2}{b^2}-1\right)}-\upsilon_2\right]\right)} \quad \text{(A4.32)}$$

Substitute equation A4.32into equation A4.30:

$$\therefore \delta_{1-2} = P_{1-2}b\left(\frac{1}{E_2(c^2-b^2)}[b^2(1-\upsilon_2)+c^2(1+\upsilon_2)]+\frac{1}{E_1(b^2-a^2)}[b^2(1-\upsilon_1)+ a^2(1+\upsilon_1)]\right) - P_{1-2}b\left(\frac{2}{E_2\left(\frac{c^2}{b^2}-1\right)\left(\frac{1}{E_3}\left[\frac{\left(\frac{d^2}{c^2}+1\right)}{\left(\frac{d^2}{c^2}-1\right)}+\upsilon_3\right]+\frac{1}{E_2}\left[\frac{\left(\frac{c^2}{b^2}+1\right)}{\left(\frac{c^2}{b^2}-1\right)}-\upsilon_2\right]\right)}\right)\left(\frac{2c^2}{E_2(c^2-b^2)}\right) - Pb\left(\frac{2a^2}{E_1(b^2-a^2)}\right)$$

$$\therefore \delta_{1-2} = P_{1-2}b\left(\frac{1}{E_2(c^2-b^2)}[b^2(1-\upsilon_2)+c^2(1+\upsilon_2)]+\frac{1}{E_1(b^2-a^2)}[b^2(1-\upsilon_1)+ a^2(1+\upsilon_1)]\right) - P_{1-2}b\left(\frac{\left(\frac{4\left(\frac{c^2}{b^2}\right)}{E_2\left(\frac{c^2}{b^2}-1\right)}\right)}{E_2\left(\frac{c^2}{b^2}-1\right)\left(\frac{1}{E_3}\left[\frac{\left(\frac{d^2}{c^2}+1\right)}{\left(\frac{d^2}{c^2}-1\right)}+\upsilon_3\right]+\frac{1}{E_2}\left[\frac{\left(\frac{c^2}{b^2}+1\right)}{\left(\frac{c^2}{b^2}-1\right)}-\upsilon_2\right]\right)}\right) - Pb\left(\frac{2a^2}{E_1(b^2-a^2)}\right)$$

$$\therefore \delta_{1-2} = P_{1-2}\left[\frac{b[b^2(1-\upsilon_2)+c^2(1+\upsilon_2)]}{E_2(c^2-b^2)}+\frac{b[b^2(1-\upsilon_1)+a^2(1+\upsilon_1)]}{E_1(b^2-a^2)}-\frac{4\left(\frac{c^2}{b^2}\right)b}{{E_2}^2\left(\frac{c^2}{b^2}-1\right)^2\left(\frac{1}{E_3}\left[\frac{\left(\frac{d^2}{c^2}+1\right)}{\left(\frac{d^2}{c^2}-1\right)}+\upsilon_3\right]+\frac{1}{E_2}\left[\frac{\left(\frac{c^2}{b^2}+1\right)}{\left(\frac{c^2}{b^2}-1\right)}-\upsilon_2\right]\right)}\right] - Pb\left(\frac{2a^2}{E_1(b^2-a^2)}\right)$$

$$\therefore P_{1-2} = \frac{\delta_{1-2}+\frac{2Pba^2}{E_1(b^2-a^2)}}{\left[\frac{b[b^2(1-\upsilon_2)+c^2(1+\upsilon_2)]}{E_2(c^2-b^2)}+\frac{b[b^2(1-\upsilon_1)+a^2(1+\upsilon_1)]}{E_1(b^2-a^2)}-\frac{4\left(\frac{c^2}{b^2}\right)b}{{E_2}^2\left(\frac{c^2}{b^2}-1\right)^2\left(\frac{1}{E_3}\left[\frac{\left(\frac{d^2}{c^2}+1\right)}{\left(\frac{d^2}{c^2}-1\right)}+\upsilon_3\right]+\frac{1}{E_2}\left[\frac{\left(\frac{c^2}{b^2}+1\right)}{\left(\frac{c^2}{b^2}-1\right)}-\upsilon_2\right]\right)}\right]},$$

δ_{1-2} is very small.

$$\therefore P_{1-2} = \frac{\frac{2P}{E_1\left(\frac{b^2}{a^2}-1\right)}}{\left[\frac{\left[(1-\upsilon_2)+\frac{c^2}{b^2}(1+\upsilon_2)\right]}{E_2\left(\frac{c^2}{b^2}-1\right)}+\frac{\left[\frac{b^2}{a^2}(1-\upsilon_1)+(1+\upsilon_1)\right]}{E_1\left(\frac{b^2}{a^2}-1\right)}-\frac{4\left(\frac{c^2}{b^2}\right)}{{E_2}^2\left(\frac{c^2}{b^2}-1\right)^2\left(\frac{1}{E_3}\left[\frac{\left(\frac{d^2}{c^2}+1\right)}{\left(\frac{d^2}{c^2}-1\right)}+\upsilon_3\right]+\frac{1}{E_2}\left[\frac{\left(\frac{c^2}{b^2}+1\right)}{\left(\frac{c^2}{b^2}-1\right)}-\upsilon_2\right]\right)}\right]}$$

$$\therefore P_{1-2} = \frac{2P}{\left[\frac{E_1\left(\frac{b^2}{a^2}-1\right)\left[(1-\upsilon_2)+\frac{c^2}{b^2}(1+\upsilon_2)\right]}{E_2\left(\frac{c^2}{b^2}-1\right)}+\left[\frac{b^2}{a^2}(1-\upsilon_1)+(1+\upsilon_1)\right]-\frac{4E_1\left(\frac{b^2}{a^2}-1\right)\left(\frac{c^2}{b^2}\right)}{{E_2}^2\left(\frac{c^2}{b^2}-1\right)^2\left(\frac{1}{E_3}\left[\frac{\left(\frac{d^2}{c^2}+1\right)}{\left(\frac{d^2}{c^2}-1\right)}+\upsilon_3\right]+\frac{1}{E_2}\left[\frac{\left(\frac{c^2}{b^2}+1\right)}{\left(\frac{c^2}{b^2}-1\right)}-\upsilon_2\right]\right)}\right]} \quad \text{(A4.33)}$$

Let: $R_1 = \frac{b}{a}, \quad R_2 = \frac{C}{b}, \quad R_3 = \frac{d}{C}$

$$\therefore \mathrm{P}_{2-3} = \frac{2\mathrm{P}_{1-2}}{\mathrm{E}_2\left({R_2}^2-1\right)\left(\frac{1}{\mathrm{E}_3}\left[\frac{\left({R_3}^2+1\right)}{\left({R_3}^2-1\right)}+\upsilon_3\right]+\frac{1}{\mathrm{E}_2}\left[\frac{\left({R_2}^2+1\right)}{\left({R_2}^2-1\right)}-\upsilon_2\right]\right)} \quad \text{(A4.34)}$$

$$\therefore P_{1-2} = \frac{\frac{2P}{E_1\left({R_1}^2-1\right)}}{\left[\frac{\left[(1-\upsilon_2)+{R_2}^2(1+\upsilon_2)\right]}{E_2\left({R_2}^2-1\right)}+\frac{\left[(1+\upsilon_1)+{R_1}^2(1-\upsilon_1)\right]}{E_1\left({R_1}^2-1\right)}-\frac{4{R_2}^2}{{E_2}^2\left({R_2}^2-1\right)^2\left(\frac{1}{E_3}\left[\frac{\left({R_3}^2+1\right)}{\left({R_3}^2-1\right)}+\upsilon_3\right]+\frac{1}{E_2}\left[\frac{\left({R_2}^2+1\right)}{\left({R_2}^2-1\right)}-\upsilon_2\right]\right)}\right]} \quad \text{(A4.35)}$$

Substitute equation A4.35 into equation A4.34:

$$\therefore \mathrm{P}_{2-3} = \frac{\frac{4P}{E_1E_2\left({R_1}^2-1\right)\left({R_2}^2-1\right)}}{\left(\frac{1}{\mathrm{E}_3}\left[\frac{\left({R_3}^2+1\right)}{\left({R_3}^2-1\right)}+\upsilon_3\right]+\frac{1}{\mathrm{E}_2}\left[\frac{\left({R_2}^2+1\right)}{\left({R_2}^2-1\right)}-\upsilon_2\right]\right)\left(\frac{\left[(1-\upsilon_2)+{R_2}^2(1+\upsilon_2)\right]}{E_2\left({R_2}^2-1\right)}+\frac{\left[(1+\upsilon_1)+{R_1}^2(1-\upsilon_1)\right]}{E_1\left({R_1}^2-1\right)}\right)-\frac{4{R_2}^2}{{E_2}^2\left({R_2}^2-1\right)^2}} \quad \text{(A4.36)}$$

For the same material of layers $E_1 = E_2 = E_3 = E$ and $\upsilon_1 = \upsilon_2 = \upsilon_3 = \upsilon$

$$\therefore P_{1-2} = \frac{\frac{2P}{\left({R_1}^2-1\right)}}{\left[\frac{\left[(1-\upsilon)+{R_2}^2(1+\upsilon)\right]}{\left({R_2}^2-1\right)}+\frac{\left[(1+\upsilon)+{R_1}^2(1-\upsilon)\right]}{\left({R_1}^2-1\right)}-\frac{4{R_2}^2}{\left({R_2}^2-1\right)^2\left[\frac{\left({R_3}^2+1\right)}{\left({R_3}^2-1\right)}+\frac{\left({R_2}^2+1\right)}{\left({R_2}^2-1\right)}\right]}\right]} \quad \text{(A4.37)}$$

$$\therefore P_{2-3} = \frac{\frac{4P}{\left({R_1}^2-1\right)\left({R_2}^2-1\right)}}{\left(\frac{\left({R_3}^2+1\right)}{\left({R_3}^2-1\right)}+\frac{\left({R_2}^2+1\right)}{\left({R_2}^2-1\right)}\right)\left(\frac{\left[(1-\upsilon)+{R_2}^2(1+\upsilon)\right]}{\left({R_2}^2-1\right)}+\frac{\left[(1+\upsilon)+{R_1}^2(1-\upsilon)\right]}{\left({R_1}^2-1\right)}\right)-\frac{4{R_2}^2}{\left({R_2}^2-1\right)^2}} \quad \text{(A4.38)}$$

The hoop stresses in the internal, middle and external layers can be obtained by the following relations:

1) For internal layer :

In equation A4.15 putting:

$P_o = P_{1-2}, \qquad P_i = P,$

$r_o = b, \qquad r_i = a.$

$$\therefore \sigma_{H1} = \frac{Pa^2 - P_{1-2}b^2 - (P_{1-2} - P)\left(\frac{a^2b^2}{r^2}\right)}{b^2 - a^2}$$

$$\therefore \sigma_{H1} = \frac{Pa^2 - P_{1-2}b^2 - P_{1-2}b^2\left(\frac{a^2}{r^2}\right) + Pb^2\left(\frac{a^2}{r^2}\right)}{b^2 - a^2}$$

$$\therefore \sigma_{H1} = \frac{Pa^2\left(1 + \left(\frac{b^2}{r^2}\right)\right) - P_{1-2}b^2\left(1 + \left(\frac{a^2}{r^2}\right)\right)}{b^2 - a^2}$$

$$\therefore \sigma_{H1} = \frac{P\left(1 + \left(\frac{b^2}{r^2}\right)\right) - P_{1-2}\left(\frac{b^2}{a^2}\right)\left(1 + \left(\frac{a^2}{r^2}\right)\right)}{\frac{b^2}{a^2} - 1}$$

$$\therefore \sigma_{H1} = \frac{P\left(1 + \frac{b^2}{r^2}\right) - P_{1-2}{R_1}^2\left(1 + \frac{a^2}{r^2}\right)}{{R_1}^2 - 1}$$

$$\therefore \sigma_{H1} = \frac{P}{{R_1}^2-1}\left(1 + \frac{b^2}{r^2}\right) - \frac{P_{1-2}{R_1}^2}{{R_1}^2-1}\left(1 + \frac{a^2}{r^2}\right) \quad \text{(A4.39)}$$

2) For middle layer:

In equation A4.15 putting:

$P_o = P_{2-3}, \qquad P_i = P_{1-2},$

$r_i = b, \qquad r_o = c.$

$$\therefore \sigma_{H2} = \frac{P_{1-2}b^2 - P_{2-3}c^2 - (P_{2-3} - P_{1-2})\left(\frac{b^2c^2}{r^2}\right)}{c^2 - b^2}$$

$$\therefore \sigma_{H2} = \frac{P_{1-2}b^2 - P_{2-3}c^2 - P_{2-3}\left(\frac{b^2c^2}{r^2}\right) + P_{1-2}\left(\frac{b^2c^2}{r^2}\right)}{c^2 - b^2}$$

$$\therefore \sigma_{H2} = \frac{P_{1-2}b^2\left(1 + \frac{c^2}{r^2}\right) - P_{2-3}c^2\left(1 + \frac{b^2}{r^2}\right)}{c^2 - b^2}$$

$$\therefore \sigma_{H2} = \frac{P_{1-2}\left(1 + \frac{c^2}{r^2}\right) - P_{2-3}\left(\frac{c^2}{b^2}\right)\left(1 + \frac{b^2}{r^2}\right)}{\frac{c^2}{b^2} - 1}$$

$$\therefore \sigma_{H2} = \frac{P_{1-2}\left(1 + \frac{c^2}{r^2}\right) - P_{2-3}{R_2}^2\left(1 + \frac{b^2}{r^2}\right)}{{R_2}^2 - 1}$$

$$\therefore \sigma_{H2} = \frac{P_{1-2}}{{R_2}^2-1}\left(1 + \frac{c^2}{r^2}\right) - \frac{P_{2-3}{R_2}^2}{{R_2}^2-1}\left(1 + \frac{b^2}{r^2}\right) \qquad \text{(A4.40)}$$

3) For external layer:

In equation A4.15 putting:

$P_o = 0, \qquad P_i = P_{2-3},$

$r_i = c, \qquad r_o = d.$

$$\therefore \sigma_{H3} = \frac{P_{2-3}c^2 + P_{2-3}\left(\frac{c^2d^2}{r^2}\right)}{d^2 - c^2}$$

$$\therefore \sigma_{H3} = \frac{P_{2-3}c^2 + P_{2-3}c^2\left(\frac{d^2}{r^2}\right)}{d^2 - c^2}$$

$$\therefore \sigma_{H3} = \frac{P_{2-3}\left(1 + \frac{d^2}{r^2}\right)}{\frac{d^2}{c^2} - 1}$$

$$\therefore \sigma_{H3} = \frac{P_{2-3}\left(1 + \frac{d^2}{r^2}\right)}{{R_3}^2 - 1}$$

$$\therefore \sigma_{H3} = \frac{P_{2-3}}{{R_3}^2-1}\left(1 + \frac{d^2}{r^2}\right) \qquad \text{(A4.41)}$$

ملخص الرسالة

المواد المركبة من المواد المتقدمة و المتاحة للإستخدام فى تطبيقات خطوط الانابيب و ايضا تمتلك نفس المواصفات السابقة.

يقدم هذا العمل دراسة سلوك الكلال للانابيب المصنوعة من الايبوكسى المدعم بالألياف الفيبر جلاس المنسوج شبكياً بإتجاهين مختلفين من التدعيم و هما [صفر،90] و [±45] و المؤثر عليه بإجهادات مركبة مكونه من عزم إنحناء (محاكاه لحمل الزلازل) و ضغط داخلى هيدروستاتيكى بنسب ضغط مختلفة (P_r) بين الضغط الفعلى المطبق على العينة ضغط الانفجار للعينة يساوى (صفر، 0.25، 0.5، 0.75) لكل الاتجاهات.

لتحسين الخواص الميكانيكية و خواص الكلال للعينات تم إستخدام طريقتين لتصنيع عينات الاختبار لكل إتجاه من اتجاهات الفيبر، ثم سوف نقوم بمقارنة نتائج الاختبارات من طريقة التصنيع الجديدة M_2 و نتائج الطريقة القديمة فى تصنيع العينات M_1.

أظهرت تجارب الحمل الثابت أن العينات ذات الإتجاه [صفر،90] كان أكثر تحملا للحمل سواء كان الثابت أو المتغير تحت تأثير عزم الإنحناء بمفرده لطرقتين التصنيع M_1، M_2. بينما كانت العينات المصنوعة بالطريقة الثانية M_2 أكثر تحملا للحمل سواء كان الثابت أو المتغير تحت تأثير عزم الإنحناء بمفرده لكل إتجاهات الفيبر. أما فى حالة الحمل سواء الثابت أو المتغير تحت تأثير عزم الالتواء بمفرده كانت العينات ذات الاتجاه [±45] الاكثر مقاومة من الاتجاه الاخر لطرقتين التصنيع M_1، M_2. بينما كانت العينات المصنوعة بالطريقة الاولى M_1 أكثر تحملا للحمل سواء كان الثابت أو المتغير تحت تأثير عزم الالتواء بمفرده لكل إتجاهات الفيبر.

أما فى حالة تجارب الظغط الهيدروستاتيكى بمفرده فقد أظهرت التجارب أن العينات ذات الاتجاه (45،-45) الاكثر تحملا للضغط الداخلى من الاتجاه الاخر لطرقتين التصنيع M_1، M_2 سواء كانت العينة ذات نهايات مفتوحة او مغلقه. بينما كانت العينات المصنوعة بالطريقة الثانية M_2 أكثر تحملا للضغط الداخلى من طريقة التصنيع الاولى M_1 لكل إتجاهات الفيبر بنسبة 40% للعينات ذات النهايه المغلقة و 45% للعينات ذات النهاية المفتوحة.

أستخدمت الصورة الاسيه ($\sigma_{max} = aN^b$) فى حالة الحمل المركب من عزم إنحناء وضغط داخلى هيدروستاتيكى أثبت انها مناسبة و ذلك بإعطاء قيم مقبولة لمعامل الارتباط. التغير فى قيم الثابت (b) لكل حالات التحميل كان مهملا حيث أعتبر ان هذا الثابت بقيمة - 0.129 للعينات المصنوعة بالطريقة الاولى M_1 و - 0.154 للعينات المصنوعة بالطريقة الثانية M_2 ، و أظهرت النتائج أن، زيادة نسبة الضغط (P_r) يسبب نقصان فى قيمة الثابت (a).

فى حالة الحمل المركب من عزم إنحناء وضغط داخلى هيدروستاتيكى تم إيجاد الإجهاد المتوسط الذى يأتى من تأثير الضغط الداخلى للعينه ووجد أنه ذو تأثير ضار على سلوك الكلال للعينة، لكل إتجاهات الفيبر و طريقتين التصنيع للعينات.

أوضحت النتائج أن الصورة المعدلة لمعادلة جودمان فى حالة الحمل المركب من عزم إنحناء وضغط داخلى هيدروستاتيكى $\left\{\frac{\sigma_H}{S_H(S_f=0)}+\frac{\sigma_{max}}{S_f(S_H=0)}=1.0\right\}_{\theta,M,P_r}$ تعبر عن تأثير الاجهادات المتوسطة وذلك لكل من إتجاهين التدعيم وأيضا لكل من طريقتى التصنيع المستخدمة فى وجود نسب ضغط مختلفة (P_r).

أختبرت صلاحية معامل SWT فى حالة الدراسة الحالية $(\sqrt{(\sigma_{max}+\sigma_m)\sigma_a})$ الذى تبين انه صالح للإستخدام ولكن يعطى قيم معامل إرتباط صغيرة لكل إتجاهات الفيبر و طريقتين التصنيع للعينات، لذلك تم تعديل معامل SWT $(\sqrt{(\sigma_{max}+\sigma_m)(\sigma_a+K\sigma_h)})$ ووجد أنه يمكن إستخدامة فى حالة الدراسة الحالية ويعطى معامل إرتباط مقبول، حيث انه يتطلب اجراء اختبار العينات تحت حمل إنحناء معكوس كلياً فقط مع استخدام معامل SWT المعدل لايجاد عمر العينات عند نسب الضغوط المختلفة. كذلك تم إختبار معامل SWT المعدل $(K_{Wafa}\sqrt{(\sigma_{max}+\sigma_m)(\sigma_a+K\sigma_h)})$ ووجد انه يساوى قيمة ثابتة تساوى 0.25489 لإتجاهى التدعيم و طريقتى التصنيع المستخدمة.

و ايضا أختبرت صلاحية معامل قياس متانة العينات فى حالة وجود إجهادات متوسطة التى تأتى من تأثير الضغط الداخلى للعينه $(\Psi=\frac{\sigma_{max}+\sigma_m}{\sigma_b})$ فى حالة الدراسة الحالية. و أوضحت النتائج أنه يمكن استخدام هذا المعامل فى حالة الدراسة الحالية.

تم التوصل إلى صورة جديدة من نظريات الانهيار لقيم نسب الضغوط المختلفة و ذلك لتوائم سلوك العينات فى حالة الدراسة الحالية مأخوذا فى الاعتبار تأثير التداخل بين الاجهادات المحلية المختلفة و كذلك التغير فى قيم النسبه (P_r) و طرق التصنيع (M) و زاويه تدعيم الالياف (θ).

تم تصميم محاكاة لايجاد عمر العينات المعرضة بإجهادات مركبة مكونه من عزم إنحناء و ضغط داخلى هيدروستاتيكى و ذلك بإستخدام ثلاث انواع من الشبكات العصبية الاصطناعية، شبكة عصبية ذات التغذية الامامية و شبكة عصبية معممة الارتداد و شبكة عصبية ذات الاساس القطرى. أوضحت النتائج ان الثلاث أنواع مناسبين لتوقع عمر الكسر للمواد المركبة. و كانت الشبكة عصبية ذات التغذية الامامية الانسب حيث انها كانت تعطى اقل خطأ.

جامعة الإسكندرية
كلية الهندسة
قسم الهندسة الميكانيكية

سلوك الكلال للإيبوكسى المدعم شبكياً بالألياف الزجاجية و المعرض لعزم إنحناء و ضغط هيدروستاتيكى

رسالة علمية

مقدمة إلى الدراسات العليا بكلية الهندسة – جامعة الإسكندرية

إستيفاء للدراسات المقررة للحصول على درجة

دكتوراه فلسفة فى العلوم الهندسية

فى

الهندسة الميكانيكية

مقدمة من

وائل عبد المنعم عبد المنعم التابعى

2014

جامعة الإسكندرية
كلية الهندسة
قسم الهندسة الميكانيكية

سلوك الكلال للإيبوكسى المدعم شبكياً بالألياف الزجاجية والمعرض لعزم إنحناء و ضغط هيدروستاتيكى

مقدمة من /

وائل عبد المنعم عبد المنعم التابعى

للحصول على درجة

دكتوراه فلسفة فى العلوم الهندسية

فى

الهندسة الميكانيكية

لجنة المناقشة و الحكم:	**موافقون**
أ.د. مصطفى ذكى محمد عبدالهادى	----------
(أستاذ بكلية الهندسة - أكاديمية الأخبار الدولية- القاهرة)	
أ.د. حسن أنور الجمل	----------
(أستاذ متفرغ بكلية الهندسة – جامعة الإسكندرية)	
أ.د. عبد الحميد إبراهيم جمعة	----------
(أستاذ متفرغ بكلية الهندسة – جامعة الاسكندرية)	

وكيل الكلية لشئون الدراسات العليا والبحوث

أ.د.هبة وائل لهيطة ----------

كلية الهندسة- جامعة الاسكندرية

لجنة الإشراف: **موافقون**

أ.د. حسن أنور الجمل ----------

(أستاذ متفرغ بكلية الهندسة – جامعة الإسكندرية)

أ.د. محمد نبيل ابو الوفا ----------

(أستاذ متفرغ بكلية الهندسة – جامعة الإسكندرية)

د. ياسر سعد محمد ----------

(مدرس بكلية الهندسة – جامعة الإسكندرية)